

Evaluation of drug-induced neurotoxicity based on metabolomics, proteomics and electrical activity measurements in complementary CNS in vitro models

Luise Schultz, Marie-Gabrielle Zurich, Maxime Culot, Anaelle da Costa, Christophe Landry, Patricia Bellwon, Theresa Kristl, Katrin Hörmann, Silke Ruzek, Stephan Aiche, et al.

▶ **To cite this version:**

Luise Schultz, Marie-Gabrielle Zurich, Maxime Culot, Anaelle da Costa, Christophe Landry, et al.. Evaluation of drug-induced neurotoxicity based on metabolomics, proteomics and electrical activity measurements in complementary CNS in vitro models. Toxicology in Vitro, 2015, 30 (1), pp.138-165. 10.1016/j.tiv.2015.05.016 . hal-02513335

HAL Id: hal-02513335

https://univ-artois.hal.science/hal-02513335

Submitted on 14 Jan 2022

HAL is a multi-disciplinary open access archive for the deposit and dissemination of scientific research documents, whether they are published or not. The documents may come from teaching and research institutions in France or abroad, or from public or private research centers.

L'archive ouverte pluridisciplinaire **HAL**, est destinée au dépôt et à la diffusion de documents scientifiques de niveau recherche, publiés ou non, émanant des établissements d'enseignement et de recherche français ou étrangers, des laboratoires publics ou privés.



Distributed under a Creative Commons Attribution 4.0 International License

Toxicology in Vitro 30 (2015) 138–165

Contents lists available at ScienceDirect

Toxicology in Vitro

journal homepage: www.elsevier.com/locate/toxinvit

Evaluation of drug-induced neurotoxicity based on metabolomics, proteomics and electrical activity measurements in complementary CNS *in vitro* models

Luise Schultz [a], Marie-Gabrielle Zurich [b], Maxime Culot [c], Anaelle da Costa [c], Christophe Landry [c], Patricia Bellwon [d], Theresa Kristl [e], Katrin Hörmann [e], Silke Ruzek [e], Stephan Aiche [f], Knut Reinert [f], Chris Bielow [f], Fabien Gosselet [c], Romeo Cecchelli [c], Christian G. Huber [e], Olaf H.-U. Schroeder [g], Alexandra Gramowski-Voss [a,g], Dieter G. Weiss [a,g], Anna Bal-Price [h,*]

[a] Department of Animal Physiology, Institute of Biological Sciences, University of Rostock, D-18051 Rostock, Germany
[b] Department of Physiology, Faculty of Biology and Medicine, University of Lausanne, Lausanne, Switzerland
[c] Laboratoire de la barrière hémato-encéphalique (LBHE) - EA2465, Université d'Artois, Faculté Jean Perrin, 62307 Lens, France
[d] Department of Toxicology, University of Wuerzburg, D-97078 Wuerzburg, Germany
[e] Department of Molecular Biology, Paris-Lodron University, Salzburg, Austria
[f] Department of Mathematics and Computer Science, Freie Universitaet Berlin, D-14195 Berlin, Germany
[g] NeuroProof GmbH, D-18119 Rostock, Germany
[h] European Commission Joint Research Centre, Institute for Health and Consumer Protection, I-21027 Ispra, VA, Italy

ARTICLE INFO

Article history:
Received 14 July 2014
Revised 26 March 2015
Accepted 18 May 2015
Available online 27 May 2015

Keywords:
In vitro blood brain barrier
MEA
Neuronal network culture
OMICs
Drug development
3D brain culture

ABSTRACT

The present study was performed in an attempt to develop an *in vitro* integrated testing strategy (ITS) to evaluate drug-induced neurotoxicity. A number of endpoints were analyzed using two complementary brain cell culture models and an *in vitro* blood–brain barrier (BBB) model after single and repeated exposure treatments with selected drugs that covered the major biological, pharmacological and neuro-toxicological responses. Furthermore, four drugs (diazepam, cyclosporine A, chlorpromazine and amiodarone) were tested more in depth as representatives of different classes of neurotoxicants, inducing toxicity through different pathways of toxicity.

The developed *in vitro* BBB model allowed detection of toxic effects at the level of BBB and evaluation of drug transport through the barrier for predicting free brain concentrations of the studied drugs. The measurement of neuronal electrical activity was found to be a sensitive tool to predict the neuroactivity and neurotoxicity of drugs after acute exposure. The histotypic 3D re-aggregating brain cell cultures, containing all brain cell types, were found to be well suited for OMICs analyses after both acute and long term treatment.

The obtained data suggest that an *in vitro* ITS based on the information obtained from BBB studies and combined with metabolomics, proteomics and neuronal electrical activity measurements performed in stable *in vitro* neuronal cell culture systems, has high potential to improve current *in vitro* drug-induced neurotoxicity evaluation.

© 2015 The Authors. Published by Elsevier Ltd. This is an open access article under the CC BY license (http://creativecommons.org/licenses/by/4.0/).

1. Introduction

Neurotoxicity testing of new compounds with the desired pharmacological effects represents one of the major bottlenecks in drug development since it is time consuming and requires large numbers of animal experiments. Indeed, neurotoxicity is one of the causes for withdrawal of pharmaceuticals from the market (Kola and Landis, 2004). Therefore, the large number of hits identified from primary high throughput discovery screens requires early,

Abbreviations: BBB, blood brain barrier; DMSO, dimethylsulfoxide; EC, endothelial cells; DIV, day *in vitro*; IPA, Ingenuity Pathway Analysis; ITS, integrated testing strategy; LY, Lucifer Yellow; MEA, micro-electrode array; RH, Ringer HEPES medium; SPSS, Statistical Package for the Social Sciences.

* Corresponding author at: European Commission Joint Research Centre, Institute for Health and Consumer Protection, Systems Toxicology Unit, Via E. Fermi 2749 TP 580, I-21027 Ispra, VA, Italy.
E-mail address: anna.price@jrc.ec.europa.eu (A. Bal-Price).
URL: http://www.ihcp.jrc.ec.europa.eu (A. Bal-Price).

http://dx.doi.org/10.1016/j.tiv.2015.05.016
0887-2333/© 2015 The Authors. Published by Elsevier Ltd.
This is an open access article under the CC BY license (http://creativecommons.org/licenses/by/4.0/).

rapid and robust preclinical screening testing strategy to assess whether compounds with desirable characteristics are neurotoxic, prior to safety and efficacy testing.

Neurotoxicity is the outcome of complex interactions of xenobiotics at the molecular, cellular and tissue level of the central and/or peripheral nervous system causing an adverse effect. An adverse effect can be caused by changes of neuronal and/or glial cell chemistry, structure and/or function. Therefore any *in vitro* testing strategy for drug-induced neurotoxicity evaluation has to be based on the combination of relevant *in vitro* models that possess the necessary molecular mechanisms and pathways that can be evaluated in a quantitative manner by sensitive, neuronal and glia-specific endpoints (Bal-Price et al., 2010; Crofton et al., 2011).

The EU 7th Framework project, Predict-IV, was established in order to develop mechanistic strategies for predictive toxicology, including neurotoxicology. The major aim of this large-scale integrated project was to provide the drug discovery community with a general test system to predict toxicity prior to pre-clinical testing. The selected compounds covered the major biological, pharmacological and toxicological responses observed in drug-induced toxicity at the level of different organs (liver, kidney and brain). One of the main criteria for the drug selection was that these three subgroups of drugs, linked to three different organs may share basic, well-known pathways, reliable biomarkers and various biochemical processes although they cause organ-specific toxicity. Thus, the selection of chemicals was based on the well documented adverse drug reactions (ADR) due to the pharmacological effect that triggers toxicity in different organs.

Based on the publicly available databases and literature search, 12 central nervous system (CNS) relevant drugs were selected to represent four different categories: (I) neuroactive and neurotoxic: CNS-drugs with strong neurotoxicity (amiodarone, buflomedil, chlorpromazine), (II) neuroactive and non-neurotoxic: CNS-drugs with no or weak neurotoxic effects (carbamazepine, diazepam, propofol); (III) non-neuroactive but neurotoxic: non-CNS drugs with significant neurotoxic effects (cisplatinum, ciprofloxacin, cyclosporine A); (IV) non-neuroactive and non-neurotoxic: non-CNS drugs with no or weak neurotoxic effects (loperamide, nadolol, ondansetron). However, these four drug groups were created only for the purpose of the electrophysiological studies to evaluate whether this end-point is sensitive enough to discriminate between drugs that are neuroactive and/or neurotoxic or non-neuroactive and/or neurotoxic after acute exposure. Among these 12 drugs four such as cyclosporine, amiodarone, diazepam and chlorpromazine were selected for an in-depth proteome and metabolome analysis. Based on the literature search amiodarone, cyclosporine and chlorpromazine should be neurotoxic and diazepam should be neuroactive but non-neurotoxic after acute exposure but could produce some toxicity after long term exposure.

Cyclosporine A and chlorpromazine were selected as they induce toxicity across different organs allowing to study whether different cell types (liver, kidney and the CNS) responded differently to the same treatment through cell specific toxicity pathways or observed toxicity was due to general cytotoxic effects. Amiodarone was selected as it produces side effects in the CNS but were originally designed for treatment of various pathologies (cardiac dysrhythmias) and diazepam was chosen because of its application as CNS drug in order to treat anxiety and seizures. Additionally, kinetics of selected drugs was studied in all three organ cultures (hepatocytes, kidney and neuronal cells) and the results obtained are described separately in this volume (e.g. Bellwon et al., 2015; Pomponio et al., 2015).

In this project we aimed to develop a novel *in vitro* approach for more comprehensive drug-induced neurotoxicity testing by providing insight into mechanisms of neurotoxicity. Since the CNS represents a high level of anatomical and physiological complexity (multiple neuronal and glial cell types) and OMICs-profiling techniques have proven to be powerful new tools (van Vliet et al., 2008; Wilmes et al., 2013) for studying complex biological processes (Csermely et al., 2013; Kleinjans, 2014; Nemes et al., 2013), in this study proteomics and metabolomics analyses were performed after long term exposure to the selected drugs. Comprehensive investigations of responses to a drug-induced perturbation on the transcriptome, proteome, and metabolome levels should lead to a better understanding of the biochemical and biological mechanisms in complex systems such as the CNS.

The study aimed for identification of possible biomarkers of neurotoxicity among the deregulated metabolites and proteins. Furthermore the OMICs analyses were combined with measurements of neuronal electrical activity after acute exposure to evaluate whether such a combination of assays will be a reliable approach for *in vitro* neurotoxicity testing. The applied endpoints were analyzed using two complementary *in vitro* brain cell cultures, cortical networks (2D) and re-aggregating brain cells (3D) after acute, sub-chronic, and repeated-exposure chronic treatments at non-cytotoxic concentrations of the selected drugs.

However, when neurotoxicity of new chemicals with unknown mechanisms of neurotoxicity has to be evaluated, firstly their possible toxicity at the blood–brain barrier (BBB) should also be considered as a fully functional BBB is of key importance for maintaining the homeostasis of the brain (Coecke et al., 2006b). Therefore the effects of 14 days of repeated treatment with the 12 selected drugs on the functionality of the BBB have been evaluated. Furthermore, the BBB is the principal route for the entry of most molecules into the CNS as well as it is the major hurdle that prevents many drugs from eliciting pharmacological or toxicological effects in the brain (Harry and Tiffany-Castiglioni, 2005). Consequently, to evaluate the neurotoxicity of compounds *in vitro* it is crucial to predict whether a drug will reach the CNS in amounts sufficient to cause toxicity. The CNS exposure is a function of several factors such as plasma protein binding, BBB permeability and brain tissue binding (Hallier-Vanuxeem et al., 2009). The ratio between the unbound concentrations in brain and plasma (Cu,br/Cu,pl) is considered as a major pharmacokinetic parameter in the CNS drug discovery (Becker and Liu, 2006; Friden et al., 2007; Kalvass and Maurer, 2002) and recently, the possibility to directly generate Cu,br/Cu,pl ratios in a single *in vitro* model of the BBB has been evaluated (Culot et al., 2013). Therefore, this alternative method has been applied here to obtain *in vitro* Cu,br/Cu,pl ratios which could then be used to estimate the Cu,br based on the plasma concentration of the studied drugs in human plasma. Based on the BBB evaluation, the estimated drug concentrations, relevant to human exposure were taken as an indication for the concentrations selected for *in vitro* neurotoxicity studies using to two mixed neuronal/glial cell culture models, mice neuronal networks (2D) and rat brain aggregates (3D).

The 2D tissue culture model of mice neuronal networks was introduced by the lab of G.W. Gross and developed over the years to a powerful tool to directly study the effects of acute exposure to test compounds effects on the electrical network communication (Gross et al., 1997). Brain region-specific networks consisting of neurons and astroglia can be cultivated for months and provide a phenotypic screening system that is being often applied in testing of both desired and unwanted effects on neuronal communication during early drug development (Johnstone et al., 2010; Lefew et al., 2013; Novellino et al., 2011).

The second mixed neuronal/glial *in vitro* model applied was a 3D rat brain aggregate model that presents a higher level of cell organization, similar to *in vivo* brain tissue cyto-architecture and function as indicated by the final ratio of neurons to glial cells, the formation of an organotypic cyto-architecture, the correct timing and extent of developmental events such as cell proliferation,

synaptogenesis, myelination and the elaboration of neuronal networks (Honegger and Zurich, 2011). This model is an excellent tool for mechanistic studies, including OMICs analysis.

It is important to stress that these two complementary mixed cell culture models (2D and 3D) contain glial cells as they are needed to maintain long-term neuronal cultures and, moreover, they are critical for toxicity response induced by a drug/chemical treatment (Bal-Price et al., 2012).

The obtained data suggest that an *in vitro* integrated testing strategy (ITS) combining information obtained from BBB studies, together with metabolomics, proteomics and neuronal electrical activity measurements performed in stable *in vitro* mixed neuronal/glial cell culture systems, has the high potential to improve current drug-induced neurotoxicity evaluation. This strategy could provide mechanistic information of altered physiological pathways that, once sufficiently perturbed, are becoming pathways of toxicity. The diversity of the applied *in vitro* endpoints and neuronal models complement each other providing an ITS with additional value to address the heterogeneity of possible toxicity mechanisms in the nervous system. The applied strategy should provide a more holistic and more efficient approach.

2. Materials and methods

2.1. Selection of the drugs

Based on the publicly available data bases and a literature search the following 12 pharmaceuticals have been selected for testing: chlorpromazine, buflomedil, amiodarone, carbamazepine, ciprofloxacin, cisplatin, loperamide, nadolol (Sigma Aldrich), diazepam (Sigma), propofol (Chemos), cyclosporine A (Calbiochem) and ondansetron (Chemos). Stock solutions were prepared in either dimethyl sulfoxide (DMSO, Sigma Aldrich, Saint Quentin Fallavier, France), water (H_2O) or HCl 100 mM (Merck Millipore, Guyancourt, France) and then diluted in cell culture medium up to previously defined, non-cytotoxic concentrations of solvents summarized in Table 1. Four drugs: cyclosporine, amiodarone, diazepam and chlorpromazine were selected for in-depth analyses for proteomics and the metabolomics performed in the neuronal/glial network cultures (2D model) and the re-aggregating brain cells (3D model) (Table 1, bold). All drugs were tested for cytotoxicity (Table 1, non bold) at two concentrations that were selected and defined as the "high" concentration, resulting in moderate cytotoxicity (10–30%) and the "low" concentration producing low cytotoxic range (0–10%).

2.2. Treatment schedules, cytotoxicity assays and selection of concentrations

2D Culture model: Concentration–response curves for lactate dehydrogenase (LDH) released into the medium, measured at days 1, 7 and 14 (cytotoxicity assays) were established for each studied drug using the LDH Cytotoxicity Detection Kit (Clonetech Laboratories, Tahara Bio Europe, France nr630117) (Fig. 1A, see also Supplemental Material Fig. SUPP 3) as this assay allowed to work with an aliquot of the supernatant and use the same cultures for the omics and electrical activity studies. Due to the limited half-life of released LDH these cannot be understood as cumulative values but only as estimates (possibly leading to an underestimation of cytotoxicity in the 7 and 14 day samples). In the control culture the cells were exposed only to medium with DMSO at the final applied concentration (1% for acute electrophysiology measurements and 0.1% for long-term treatments for metabolomics and proteomics).

At each time point of medium change (6 well plates, 1×10^6 cells/well) 350 µl of the supernatant were collected, transferred to a 1 ml Eppendorf tube to determine the LDH content. This assay was applied because it allowed further cultivation and taking of

Table 1
Drugs tested and the concentrations used in the experiments for the different *in vitro* models.

Drugs[a]	2D Neuronal networks	3D Brain cell aggregates	Blood brain barrier (µM)[b]	Group[c]
Amiodarone antiarrhythmic also hepatotoxic	**Low: 0.0035 µM** **Medium: 0.350 µM**[d] **High: 1.25 µM**[d]	**Low: 0.125 µM** **High: 0.625 µM**	5	I. Neuroactive and neurotoxic
Chlorpromazine sedative also hepatotoxic	**Low: 0.01 µM** **High: 2.5 µM**	**Low: 0.2 µM** **High: 1 µM**	2	I. Neuroactive and neurotoxic
Buflomedil vasoactive	Low: 0.01 µM High: 6.25 µM		2	I. Neuroactive and neurotoxic
Diazepam tranquillizer	**Low: 100 pM** **High: 0.01 µM**	**Low: 0.3 µM** **High: 1.5 µM**	5	II. Neuroactive and non-neurotoxic
Carbamazepine anticonvulsant	Low: 2.5 µM High: 20 µM		40	II. Neuroactive and non-neurotoxic
Propofol anesthetic	Low: 0.001 µM High: 6.4 µM		25	II. Neuroactive and non-neurotoxic
Cyclosporine A immunosuppressive also nephrotoxic	**Low: 0.1 µM**[a] **High: 2 µM**	**Low: 0.2 µM** **High: 1.0 µM**	1	III. Non-neuroactive and neurotoxic
Cisplatinum antineoplastic also nephrotoxic	Low: 1 nM High: 1 µM		15	III. Non-neuroactive and neurotoxic
Ciprofloxacin antibiotic	Low: 12.5 µM High: 100 µM		10	III. Non-neuroactive and neurotoxic
Loperamide antidiarrhoeal	Low: 100 pM High: 10 µM		0.01	IV. Non-neuroactive and non-neurotoxic
Nadolol antihypertensive	Low: 10 nM High: 10 µM		1	IV. Non-neuroactive and non-neurotoxic
Ondansetron antiemetic	Low: 1 nM High: 30 µM		1	IV. Non-neuroactive and non-neurotoxic

[a] The bold labeled drugs and concentrations were used for the OMICs experiments, the non-bold ones for cytotoxicity measurements. Electrophysiology measurements were performed on a wider concentration range).
[b] Clinically relevant concentrations used in BBB experiments.
[c] Preliminary assignment to the four groups.
[d] Because of the detection limit for amiodarone by HPLC–MS, a second higher concentration was studied.

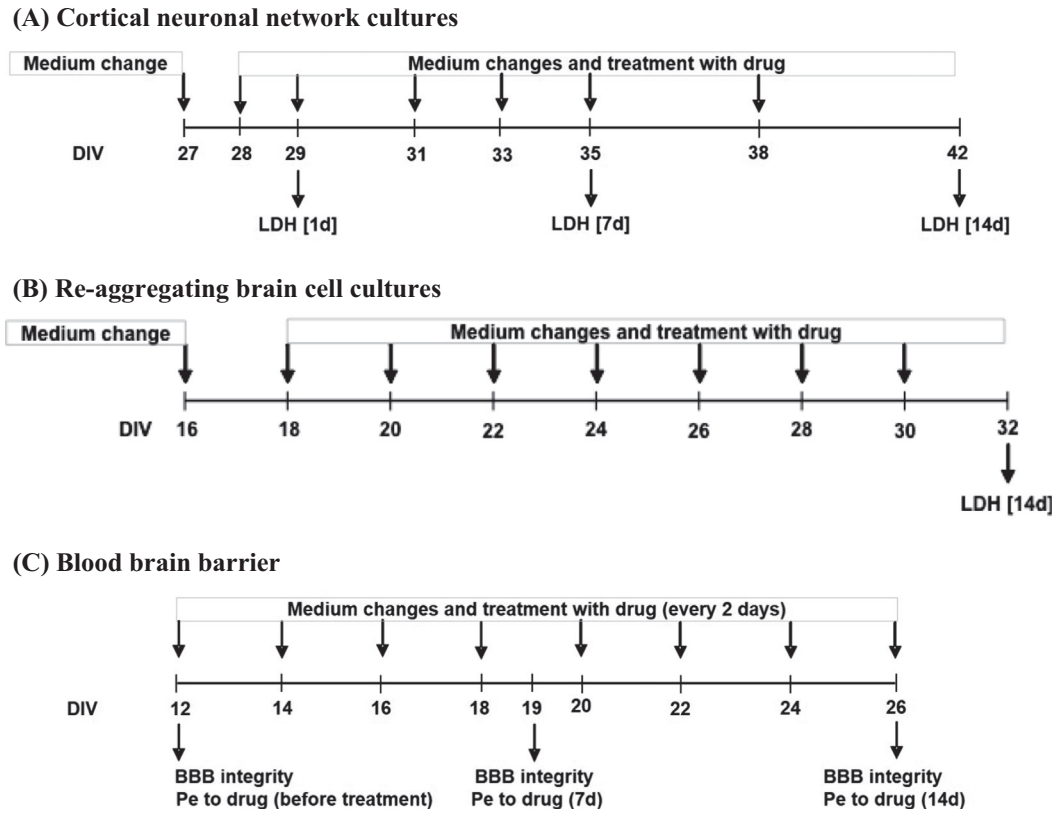


Fig. 1. Scheme of treatments and LDH determination: (A) 2D neuronal networks (released LDH was determined in cell culture medium) and (B) 3D aggregates (an intracellular LDH activity.

aliquots from the very same culture for additional assays including the proteomics study. Cultures treated with TritonX 100 which resulted in complete release of LDH were used as positive control. The collected sample tubes were centrifuged to remove cell debris. Samples of 100 µl were transferred to a 96well plate (3 technical repeats). The reaction mixture was be prepared by adding and gently mixing to avoid foam. Then 100 µl Reaction Mixture (250 µl of Catalyst with 11.25 ml of Dye Solution for 100 tests) were added and incubated at room temperature for 30 min. The enzymatic reaction was stopped by adding 50 µl of 1 N HCl and the samples' absorption was read at 490 nm in a microplate reader (iMarkTM, Bio Rad). Data were exported with MPM6 software and statistically processed. Means were calculated for all technical triplicates and the biological replicates. Data were normalized to positive controls (100% lysis with TritonX100) and effects of DMSO were eliminated by solvent-only treated controls. The values shown describe the concentration-dependent percentage of released LDH into the culture medium at the defined timepoints (Fig. 2A).

For 3D aggregate cultures intracellular LDH activity (Fig. 2B) was measured by a conventional photometric assay (Koh and Choi, 1987) after 14 days of exposure to the studied drugs. Control cultures received the equivalent amount of the solvent (DMSO). Intracellular LDH activity, extracellular LDH release and glucose consumption were not affected by a 7-day exposure to concentrations of DMSO ranging from 0.1% to 0.8%. For more safety, a concentration of 0.05% of DMSO was chosen for all experiments. All data are expressed as percentage of control cultures containing the carrier medium only. They are the mean of 9 replicates coming from three biological repeats.

For the BBB model LDH measurements were not perfomed but DMSO without drug was used as a control and it was verified that the final DMSO concentrations used did not affect the tightness of the barrier. The scheme of treatment for the BBB model was as follows: treatments with drugs were initiated after 12 days of endothelial cells co-cultured with glial cells to induce cell differentiation (D0–D12). Medium and treatments were renewed every 2 days from DIV 12 to DIV 26. Before and after 7 or 14 days of repeated dose treatment with drugs, the permeability (Pe) of the BBB to the drugs was assayed and the integrity of the BBB monitored by the permeability of a fluorescent marker molecule, Lucifer Yellow (Fig. 1C).

For subsequent studies of metabolomics and proteomics two concentrations were chosen based on the LDH assay, the "low" which was in the low or non-cytotoxic range and the "high" in the moderate cytotoxicity range (10–30%). For the 3D model the lower concentration was 1/5 of the high concentration. The lower concentration was further reduced when the electrical activity patterns were already impaired at this concentration (final concentrations see Table 1).

For the measurement of the electrical activity, concentration curves were determined based on 8 or more increasing concentrations to obtain the entire concentration–response curve for each drug. At higher concentrations of the drugs both cytotoxic and neurotoxic effects were expected.

For *in vitro* BBB model the concentrations of each drug, relevant to their therapeutic total plasma concentrations (Ct, pl) in humans (Table 1) were applied to the luminal compartment of the model (Fig. 3), mimicking the blood compartment.

2.3. Establishment and maintenance of the in vitro BBB model

To establish *in vitro* BBB model the method of Dehouck et al. (1990) was used with minor modifications. Capillaries were isolated from bovine brain cortex according to the homogenization technique from Meresse et al. (1989). After seeding of microvessel

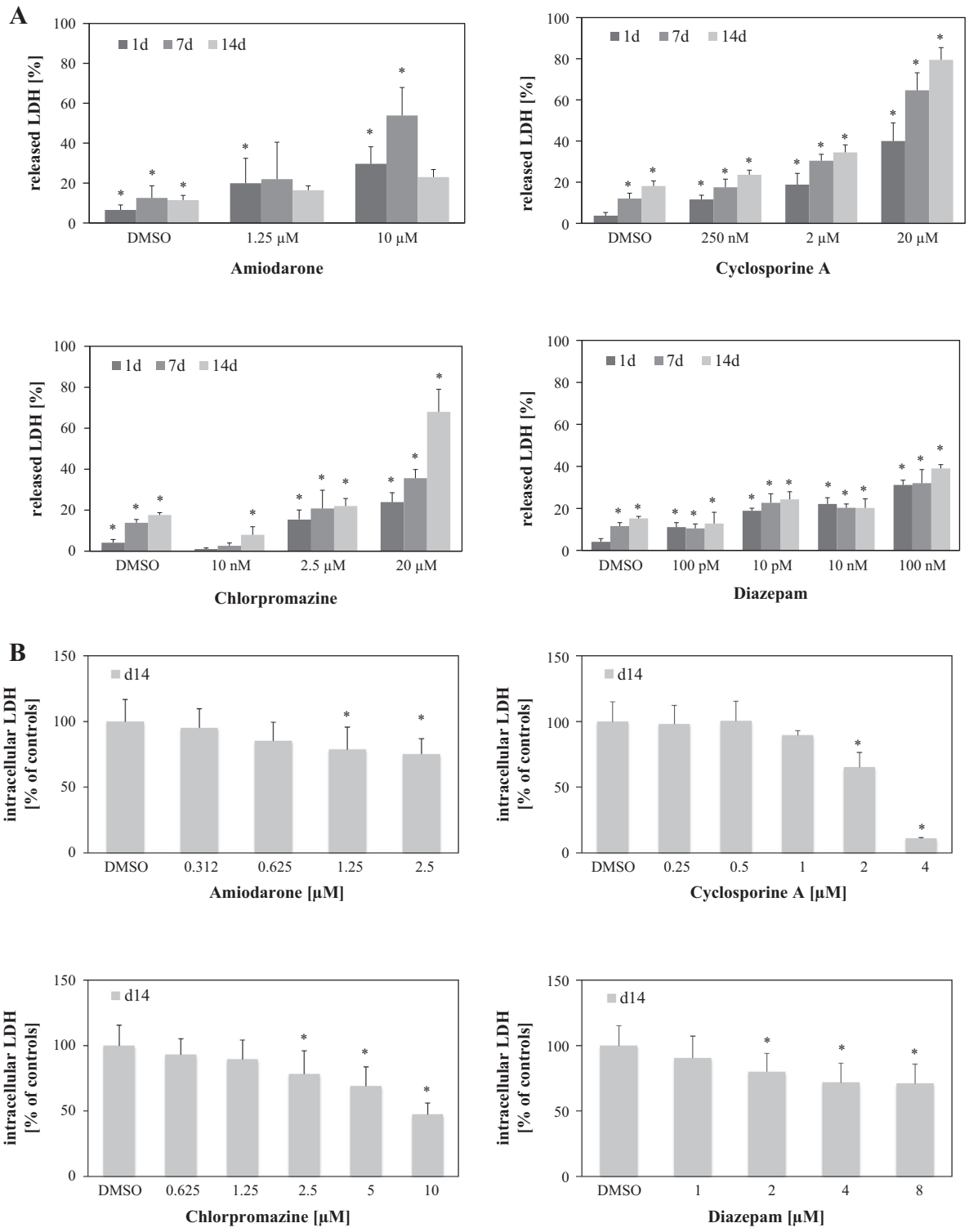


Fig. 2. Concentration-dependent changes of LDH, reflecting cytotoxicity, determined upon exposure to drugs by (A) extracellular, released LDH measured in the medium of the 2D neuronal/glial networks after 1, 7 and 14 days of exposure to four tested drugs and DMSO (0.1%) expressed as percentage of total LDH release induced by Triton X100 and B: intracellular LDH activity determined in the 3D model after 14 days (expressed as % of control) of treatment with the four studied drugs and DMSO (0.05%). For both models the significance was determined with ANOVA followed by Tukey posthoc test ($^*p \leqslant 0.05$).

extract on extracellular matrix-coated dishes, microcolonies of endothelial cells (ECs) migrating from seeded capillaries were harvested by selective trypsinization and sub-cultured before storage in liquid nitrogen. This procedure enables pure capillary endothelial cell cultures to be obtained which are then co-cultured for 12 days with primary mixed glial cells to obtain a reliable *in vitro* model of the BBB. Glial cells were isolated from newborn (3 days old) Sprague–Dawley rats according to the method of Booher and Sensenbrenner (1972) and plated on the bottom of six well plates at a concentration of 1.2×10^5 cells/mL in 2 mL of DMEM

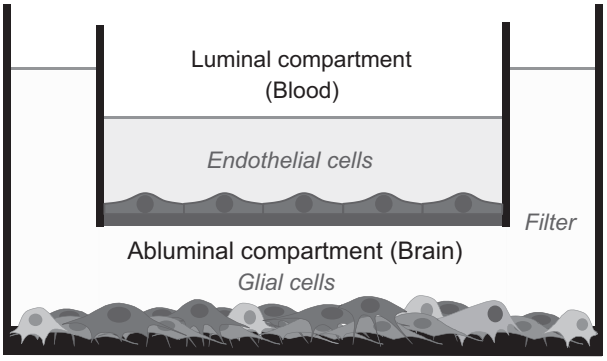


Fig. 3. Schematic representation of the *in vitro* BBB model with the two compartments representing the blood and the brain space. Bovine brain capillary endothelial cells (ECs) were seeded on the upper side of the filter and primary rat glial cells at the bottom of the well. After 12 days of EC co-culture with glial cells to induce endothelial cell differentiation, drug treatments in the luminal compartment were initiated and renewed every 2 days for up to 14 days of exposure.

supplemented with 10%(v/v) fetal calf serum. The medium was changed twice a week and after 3 weeks of culture the glial cells were used for co-culture.

The ECs were seeded on collagen-coated cell culture inserts, which were placed in the wells containing glial cells (schematic representation of the *in vitro* BBB model in Fig. 3). The medium used for the co-culture was Dulbecco's modified Eagle's medium (DMEM, Life Technologies, Saint Aubin, France) supplemented with 10% (v/v) newborn calf serum (CS, Integro b.v., Zaandam, The Netherlands), 10% (v/v) horse serum (HS, Life technologies), 2 mM glutamine (Sigma Aldrich), 50 μg/ml gentamycin, and 1 ng/ml of basic fibroblast growth factor (bFGF, Sigma Aldrich). The medium was changed every second day. Under these conditions, ECs formed a confluent monolayer after 5 days. Treatments were initiated 7 days after confluence was reached.

2.3.1. In vitro BBB model: drug treatment regime

For *in vitro* BBB experiments, all tested drugs were solubilized in dimethyl sulfoxide (DMSO, Sigma Aldrich, Saint Quentin Fallavier, France), except buflomedil and ciprofloxacin (Merck Millipore, Guyancourt, France) which were solubilized in water or 100 mM HCl respectively. To avoid any unwanted toxicological effects of a solvent, these stock solutions were then further diluted in cell-culture medium to the final non-cytotoxic concentration of 0.25% DMSO and 0.25% HCl (v/v).

After 12 days of co-culture (endothelial with glial cells), diluted drug stock solutions were added to co-culture medium in the luminal compartment of inserts. The abluminal compartment containing glial cells was filled with fresh medium. In the case of repeated treatment, media were refreshed and treatment renewed every 2nd day. As controls, ECs were treated with 0.25% of the different solvents (H_2O, DMSO, HCl) without drugs.

Initially *in vitro* models of the BBB have been used to assess the rate of transport (permeability) across the BBB, however for predicting neurotoxicity following repeated administration, the rate of transport may not be critical. Based on the hypothesis, that only the unbound brain concentration (Cu,br) is available for interaction with the majority of CNS receptors, it may be essential to determine Cu,br of drugs. Recently, the possibility to use a co-culture of brain capillary endothelial and glial cells in an attempt to mimic the *in vivo* situation and to predict Cu,br/Cu,pl ratios *in vitro* has been demonstrated (Culot et al., 2013). Therefore, this alternative method has been used here to obtain *in vitro* Cu,br/Cu,pl ratios that could then be used to estimate the Cu,br based on the plasma concentration of the studied drugs determined in human plasma.

2.3.2. Evaluation of in vitro BBB integrity and permeability to drugs (Pe) measurements

Briefly, after 7 and 14 days of repeated treatment the filters containing monolayers of endothelial cells were transferred to six-well plates containing 2.5 ml of Ringer-HEPES (RH) solution (150 mM NaCl, 5.2 mM KCl, 2.2 mM $CaCl_2$, 0.2 mM $MgCl_2(6H_2O)$, 6 mM, $NaHCO_3$, 5 mM HEPES, 2.8 mM glucose, pH 7.4) per well. 1.5 ml RH solution containing the drug at a single pre-selected concentration (Table 1) and 20 μM of the integrity marker Lucifer Yellow (LY) were added to the cell monolayer and the plates placed on an orbital shaker at 37 °C. After 1 h, aliquots were taken from both compartments and the amount of drug and fluorescent tracer i.e. Lucifer Yellow (LY) were determined by LC/MS and fluorescence spectrophotometry (Synergy H1, Biotek, Winooski USA), respectively.

The endothelial permeability coefficients (Pe) were calculated in centimeters per minute. In this calculation, the cleared volume was calculated, as described by Siflinger-Birnboim et al. (1987), by dividing the amount of compound in the receiver compartment by the drug concentration in the donor compartment at each time point. The average cumulative volume cleared was plotted vs. time and the slope was estimated by linear regression analysis (EXCEL 5.0) to give the mean and standard deviation of the estimate. The slope of the clearance curve with inserts alone and inserts with cells is equal to PSf and PSt respectively, where PS is the permeability surface area product. The units of PS and S are in microliters/minute and square centimeters, respectively. The PS-value for the endothelial monolayer (PSe) was computed as follows: $1/PSe = 1/PSt - 1/PSf$. To generate the endothelial permeability coefficient, Pe ($cm\ min^{-1}$), the PSe-value was divided by the surface area of the insert (i.e. 4.7 cm^2).

To assess possible adsorption to plastics or non-specific binding to cells, the mass balance (%) was calculated from the amount of compound recovered in both compartments at the end of the experiment divided by the total amount added in the donor compartment at 0 min. Pe values were not calculated for compounds with a mass balance value below 75%. After BBB integrity was evaluated, cell culture inserts were placed back in the wells and fresh medium was added.

A drug was considered to induce a toxic response (impairment of the functionality of the BBB) when the Pe to LY value of treated cells was significantly higher than the one of control cells (i.e. non-treated cells or cells treated with solvent only at the same time-point) (Culot et al., 2008; Hallier-Vanuxeem et al., 2009).

2.3.3. Evaluation of brain/plasma ratio of free drug using the in vitro BBB model and prediction of unbound brain concentration

After different time of exposures, co-cultures of ECs and rat glial cells were rinsed 3 times with RH solution. The abluminal compartments containing the glial cells were filled with 2.5 ml of RH solution. Then, 1.5 ml of test drug-containing solution and 20 μM of LY in RH solution were added to the luminal compartment. After 1 h of incubation in a shaker at 37 °C with a low shaking velocity, aliquots from the donor and receiver compartment were taken and analyzed. Results were used only when Pe to LY indicated that the integrity of the monolayers was maintained for the duration of the transport experiment with drug (i.e. no significant difference vs. Pe to LY in non treated cells).

The mean free brain/plasma ratios were calculated from three individual experiments for each drug. One hour ratios were calculated by dividing the free drug concentration in the receiver compartment by the free drug concentration in the donor compartment after 1 h. The experimental data at one hour (i.e. concentration in both compartments at the beginning of the experiment and after 1 h) were computed using the blue-norna® steady-state calculator (www.blue-norna.com) to predict the

in vivo steady-state Cu,br/Cu,pl ratios. For further details on this calculation method see Culot et al. (2013).

The total therapeutic concentrations of drugs found at steady-state in human plasma (i.e. derived empirically from studies in which optimal therapeutic effects were achieved and side effects were minimized for the majority of patients) reported by Lafuente-Lafuente et al. (2009) for amiodarone, Sadeque et al. (2000) for loperamide and Regenthal et al. (1999) for all other studied compounds were used. The data on drug binding to plasma proteins were retrieved from the literature or from public resources such as DrugBank (http://drugbank.ca/), and DailyMed (http://dailymed.nlm.nih.gov/dailymed/about.cfm).

To estimate the concentration unbound in human plasma (Cu,pl), the total plasma concentrations of drugs found in human plasma (Ct,pl) were multiplied by the unbound fraction in human plasma (fu,pl) (Eq. (1): Cu,pl = Ct,pl ∗ fu,pl). The Cu,br values were then estimated by multiplying the Cu,pl by the predicted steady-state Cu,br/Cu,pl ratios obtained from the *in vitro* BBB model (Eq. (2): Cu,br = Cu,pl ∗ steady-state Cu,br/Cu,pl).

2.4. Preparation and maintenance of neuronal network cultures from murine embryonic cortex (2D model)

Primary cell cultures were prepared from the brain cells extracted from embryonic CNS tissue. The frontal cortex was harvested from embryonic NMRI mice (Charles River, Sulzfeld, Germany) at day 15–16. The animals were sacrificed by cervical dislocation according to the German Animal Protection Act §4. The tissue was enzymatically dissociated with a mixture of Papain (Roche Diagnostic GmbH, Mannheim, Germany) and DNase (Roche Diagnostic GmbH, Mannheim, Germany) as well as mechanically with transfer pipettes and cultured according to the basic methods established by Ransom et al. (1977) with minor modifications such as the use of DNase I (8000 U/ml) and papain (10 U/ml) for dissociation which were applied to the cells for 15 min at 37 °C (Huettner and Baughman, 1986). The cells were re-suspended in supplemented primary neurobasal medium (PNB medium with PNGM Singlequot Kit; Lonza Sales AG, Verviers, Belgium) at a density of 1×10^6 cells/ml. The MEAs and 6 well plates were treated slightly differently: before cell seeding each electrode array on the MEA was covered with 100 µl poly-D-lysine for 24 h at 37 °C (removed and washed twice with *aqua ad injectabilia*) and left to dry. Then, prior to the cell seeding, laminin (50 µl) was applied to each array for 3 h at 37 °C. The total seeding volume for each array was 300 µl with a cell density of 1×10^6 cell/ml (Gramowski et al., 2004; Gross et al., 1993) filled up to 2.5 ml after 2 h at 37 °C. The cell cultures on 6 well plates for OMICs were also covered with poly-D-lysine (1.5 ml) for 24 h at 37 °C but in contrast to the MEAs, the plates did not get the laminin treatment. The seeding volume for each well was 2 ml with a cell density of 0.5×10^6 cells/ml. Toxicity testing experiments in the 2D model started at 28 day *in vitro* (DIV). Culture medium was replenished three times a week with serum free media. The cortical network cultures contain a variety of neurons (∼20%) and astrocytes (∼70–80%), few microglia cells (∼1–2%) but only negligible numbers of oligodendrocytes. Neurons are able to differentiate with the formation of synapses and with the brain-region specific pharmacological characteristics (Gross and Gopal, 2006; Johnstone et al., 2010; Weiss, 2011) but do not form myelin sheaths.

The glial cells have an important supportive function for the metabolism and for supplying the neurons with ions and nutrients. Therefore, the neuronal networks with glial cells are stable for several months (Gramowski et al., 2006). While neuronal cells are post-mitotic, glial cells are allowed to proliferate for 3–5 days up to a certain density (about 80% of the surface area). To prevent overgrowth of glial cells the developing cultures received a single treatment of 5-fluoro-2′-deoxyuridine (25 µM, Sigma–Aldrich, Taufkirchen, Germany) at day 4. This treatment is not cytotoxic for the development of functional neuronal networks and their connectivity (Keefer et al., 2001; Ransom et al., 1977)

2.5. Preparation and maintenance of the re-aggregating brain cell cultures (3D model)

Rotation-mediated aggregating cell cultures were prepared from 16-day fetal Sprague–Dawley rat brains (Janvier Laboratories, France) as previously described in detail (Honegger and Zurich, 2011). Briefly, the dissected brain tissue, comprising the telencephalon, mesencephalon and rhombencephalon, was dissociated mechanically using nylon sieves of 200- and 115-µm pores. The dissociated and washed cells were re-suspended in serum-free modified DMEM (Honegger and Zurich, 2011). Aliquots of the cell suspension (containing the amount of cells obtained on average from one fetal brain) were transferred to culture flasks, and maintained under constant gyratory agitation at 37 °C in an atmosphere of 10% CO_2 and 90% humidified air. Media were replenished by replacing 5 ml of medium (of a total of 8 ml) with 5 ml of fresh medium at intervals of 3 days until 14 DIV, and at intervals of 2 days thereafter. These rotation-mediated cultures form even-sized spherical structures composed of all the different types of neuronal and glial cells (astrocytes, oligodendrocytes and microglial cells), and adult-like neural progenitors (Zurich and Honegger, 2011). The 3D structure permits numerous cell-to-cell interactions, as well as the exchange of soluble factors, allowing cells to differentiate in a histotypic fashion, i.e. with the formation of synapses, compact myelin and extracellular matrix (Honegger et al., 1979; Monnet-Tschudi et al., 1993. Finally, the constant gyratory agitation assures sufficient oxygenation and nutrient supply.

2.6. Drug treatment and sample preparation for metabolomics and proteomics analyses

The cells of the 2D (at 28 DIV) and 3D cultures (at 18 DIV) were treated for 1, 3 or 14 days with the selected low or high concentration based on the LDH cytotoxicity assay (see Section 2.2) of the four compounds (in bold, see Table 1). The samples for the metabolomics and proteomics studies were prepared following a common protocol for the 2D and the 3D culture model.

2.6.1. Sample preparation from neuronal network cultures from murine embryonic cortex (2D model)

For metabolomics and proteomics studies cells were seeded at a cell number of 1×10^6 cells/well in six-well plates. Before cell seeding the wells were treated with poly-D-lysine (30–70kD, Sigma–Aldrich, 25 µg/ml) for 24 h, then washed twice with *aqua ad injectabilia* and covered with laminin (16 µg/ml, Roche Mannheim, Germany). The cultures were fed with serum-free Neurobasal medium (supplemented with PNGM Singlequot Kit; both from Lonza Sales AG, Verviers, Belgium) three times a week for 28 days and one day before treatment. Cells were treated with the four selected drugs (bold in Table 1, low and high concentration).

For sample preparation neuronal network cultures were washed in PBS and scraped in methanol. The cells from two wells were pooled (approximately 1.5 ml of total volume of isolated cells) briefly vortexed and sonicated on ice. After centrifugation the supernatant was transferred into pre-cooled Eppendorf tubes for subsequent metabolite analysis by NMR spectroscopy (metabolomics) and the remaining cell pellets were analyzed by HPLC–mass spectroscopy for peptide fingerprinting (proteomics).

2.6.2. Sample preparation from re-aggregating brain cell cultures (3D model)

For the preparation of the replicate cultures, the free-floating aggregates in 4 original flasks were pooled and redistributed in 1-ml aliquots to culture flasks containing 7 ml of fresh pre-equilibrated culture medium. After their preparation, replicate cultures were equilibrated for 2 h under normal culture conditions prior to the addition of the drug. The stock solutions of the four studied drugs (in bold, Table 1) were prepared in DMSO. For the treatment of the cultures, aliquots of the stock solutions (2000-fold concentrated) were added directly to the culture supernatants, starting at 18 DIV. Then, after each medium replenishment (5 ml out of 8 ml), aliquots of stock solutions were added to the culture supernatants in order to compensate for the fresh medium added. Control cultures received an equal volume of the solvent. For each chemical, 3 independent experiments were performed, using each time a new culture preparation in order to have three replicates per group. The cultures were harvested for analysis after 1, 3 and 14 days of exposure to the drugs. Then samples were prepared for metabolomics and proteomics, as follows. The content of each flask was transferred into a sterile 15-ml plastic tube placed on ice. The aggregates settled by gravity were washed 2× with PBS. After PBS removal, 1 ml ice-cold methanol (LC–MS Chromasolv, Riedel-de-Haën) was added. After sonication on ice, the homogenates were transferred in an Eppendorf tube previously washed with methanol and centrifuged at 4 °C, 12 min, 16,000*g*, in a pre-cooled centrifuge. The supernatants were recovered in an Eppendorf tube previously washed with methanol for metabolomics (NMR) analysis. The cell pellets were used for proteomics. Samples were immediately transferred in dry ice, and then stored at −80 °C.

2.6.3. Metabolomics: processing of samples and data analysis

For the analysis of the cellular metabolome, a non-targeted analysis were carried out by recording high resolution ^{1}H NMR spectra of hydrophilic cell extracts at 600 MHz without preseparation on a Bruker DMX 600 spectrometer equipped with a 5 mm DCH cryoprobe (both by Bruker Biospin GmbH, Rheinstetten, Germany). Water suppression was achieved by use of the NOESYGPPR1D-pulse program from the Bruker library. For Fourier transformation, 256 scans and 16 dummy scans with an acquisition time of 4.95 s were recorded in the non-spin-mode. Spectral width is 13227.5 Hz. Instrument control, data recording and baseline correction were carried out on Bruker WIN-NMR Suite. ^{1}H NMR spectra were inspected visually to exclude any outliers due to inadequate water suppression or baseline distortions.

Basic multivariate data analysis and a database comparison of the peaks was performed and all metabolites were identified using the Profiler™-function and the compound library of Chenomx NMR Suite (Chenomx Inc.) as described before (Sieber et al., 2009). Values are presented as fold changes per sample pair (treated vs. medium control containing carrier only and cultured under identical conditions for the same time). Significance was tested by 2 way ANOVA with Bonferronis posttest; values with $p > 0.05$ where excluded.

2.6.4. Proteomics: processing of samples and data analysis

For the proteomics analysis treated cells were lysed in ice cold 100% methanol to stop enzymatic activities. The protein measurements and identification were performed by HPLC–MS following the procedure described by Wang et al. (2005) with modifications as described by Wilmes et al. (2013). Briefly, in preparation for the measurement with HPLC–MS the peptides were labeled with iTRAQ. The basis for the iTRAQ quantification were the reporter ions extracted from HCD spectra. To identify the peptides separate searches for CID (collision-induced dissociation) and HCD (higher energy collisional dissociation) spectra were made against an interfaced version of SwissProt Database on multiple search engines including Mascot, OMSSA and XTandem. To ensure that only unique peptide hits were shown, an ensuing false discovery rate (FDR, filtering at 5%) approach using a decoy database was performed.

The HPLC instrument was a U3000 nano HPLC Unit from Dionex (Germering, Germany) and the mass spectrometer was an LTQ Orbitrap XL from Thermo Fisher Scientific equipped with a nano-electrospray ion source. The samples were measured with a Nano-ion-pair reversed-phase (IP-RP) – HPLC at pH 2 and an LTQ-Orbitrap-MS. The flow rate was set to 1 μL/min and a monolithic 150 × 0.2 mm I.D. column, commercially available as PorSwift™ columns from Dionex, Part of Thermofisher) was used for the separation. A 5 h gradient of 0–40% acetonitrile in 0.050% aqueous trifluoroacetic acid was applied. To quantify peptides, which were labeled with iTRAQ, three data-dependent CID scans were executed.

Tandem-MS spectra were acquired in CID (collision-induced dissociation) and HCD (higher-energy collisional dissociation) mode for all selected precursor ions. Each sample was measured in triplicate using exclusion lists, i.e. after the first run the Raw file was sent to Proteome Discoverer to generate a list of all precursor *m*/*z* values which were already identified. For the second run the exclusion list, which was created after the first run, was added to the instrument method. With the exclusion list it was possible to avoid the fragmentation of all precursor ions, which were already identified in the run before. For the third run both Raw files from the previous runs were used to create the exclusion list. This procedure facilitated the identification of more proteins compared to using a single measurement. Identification and quantification of proteins were performed using an integrated pipeline of OpenMS (Sturm et al., 2008) and the isobar package (Breitwieser et al., 2011). For identification, a consensus approach was used, i.e., the data was analyzed by multiple identification engines: X! Tandem 2009.04.01.1 (Craig and Beavis, 2004), OMSSA 2.1.9 (Geer et al., 2004), Mascot v2.3 (Perkins et al., 1999). The results were combined using the Consensus ID approach (Nahnsen et al., 2011). A 5% false discovery rate (FDR) for peptides was enforced using a target-decoy approach. For peptide quantification the OpenMS tool iTRAQAnalyzer was used to extract the quantitative information from HCD spectra and correct for isotopic impurities applying a non-negative least squares procedure (NNLS). The resulting quantitative information was subsequently mapped back to the previously acquired identification data for subsequent protein quantification using the isobar software package (Breitwieser et al., 2011). iTRAQ channels were normalized based on median of pairs normalization. Protein ratios were computed (after outlier elimination) from unique peptides only using a weighted average based on peptide noise level. Values are obtained as fold changes per sample pair (treated vs. carrier medium control, cultured under identical conditions). Significantly increased or decreased proteins are reported if two p-values are below 0.05: the first *p*-value is based on a Cauchy distribution fitted to the global protein ratio distribution, the second on the spread of peptide ratios contributing to the protein ratio (see Breitwieser et al., 2011 for details).

The IPA (Ingenuity Pathway Analysis) software was applied to create from a list of differentially-expressed proteins and their gene/protein ID numbers information on the biological networks possibly associated with these proteins (http://www.ingenuity.com). The program uses a knowledgebase derived from the scientific literature to relate genes or proteins based on their interactions and functions. IPA generates information on biological networks, canonical pathways and functions relevant to the dataset. Highly regulated biological networks and functions were identified using association rules among focus genes/proteins. Raw

data were processed with Excel and subsequently analyzed with IPA. The raw data were converted from log10 to log2 and a p-value of 0.05 (log ratio 1.5) was applied as threshold.

2.7. Measurement of electrical activity in neuronal network cultures from frontal cortex (2D model)

2.7.1. Recording spontaneous electrical activity in control and treated cultures

The neuronal cultures grow as self-organized neural networks which consist of a mixture of different neuronal cell types and glial cells, directly on the micro-electrode array (MEA). The neurons couple electrically to the neurochip electrodes whereby the action potentials (spikes) of the cells can be recorded extracellularly. The network cultures start to develop spontaneous electrical activity after 3–5 days *in vitro* in the form of random spiking. During the 4 weeks in culture, the activity pattern is stabilizing and changes into a synchronized pattern consisting of coordinated bursting and interburst spiking (Gramowski et al., 2010, 2004).

The MEA neurochips were provided by the Center for Network Neuroscience (University of North Texas, Denton, TX, USA). The dimension of the chip is $5 \times 5\,cm^2$ with a $2.1\,mm^2$ recording matrix in the center with 32 passive electrodes and indium tin oxide conductors. The hydrophobic insulation material was activated by a short flaming (butane) through a stainless steel mask and subsequent treatment with poly-D-lysine and laminin. Thus, cell adhesion was ensured within a defined, adhesive area only.

For recording, the MEAs were placed into a sterilized recording chamber and maintained at 37 °C. The recordings were made in serum-free medium and the pH was kept constant at 7.4 with a continuous stream of filtered, humidified air with 5% CO_2. Recording was performed with a computer-controlled 64-channel MEA workstation data acquisition system (Plexon, Inc., Dallas, TX, USA) providing amplification, filtering (3 Hz–7 kHz), and digital signal processing of MEA signals. The total system gain used was 10 K with a simultaneous 40 kHz sampling rate. The signals routinely recorded by these neurochips are in the range of 15–1800 μV. For obtaining concentration response curves and effective concentration, EC_{50}-values, first the networks native activity was recorded for 1 h. Then cultures were exposed acutely to at least nine accumulating concentrations of the same drug and recorded for 30 min when after 15 min a stable pattern had developed. Recordings were taken from at least 3 biological repeats from which 4 to 8 concentration series were analyzed for each of the 12 drugs investigated: amiodarone, buflomedil, chlorpromazine, carbamazepine, diazepam, propofol, cisplatinum, ciprofloxacin, cyclosporine A, loperamide, nadolol, and ondansetron. The network response (spike rate) was observed online.

2.7.2. Multi-parametric data processing

To obtain quantitative data from the one-hour recordings for each of 8 or more concentrations over a wide range, stable activity phases of the last 30 min were selected for evaluation. The multichannel signal acquisition system delivered single neuron action potential (spike) data including their waveforms. Spike identification and separation were accomplished using a template-matching algorithm in real time. This permitted the simultaneous extracellular recording of action potentials from up to 128 neurons. The spikes were recorded as spike trains which include clusters, so-called bursts which were quantitatively described via direct spike train analysis using NPWaveX (NeuroProof GmbH, Rostock, Germany). This yields a description of the pattern characteristics consisting of 200 parameters belonging to five general categories:, burst structure, oscillation, synchronization, connectivity and general activity. For direct comparability all parameters were normalized for each experiment and each experimental treatment with regard to the corresponding values of the native reference activity. This multiparametric description of the network activity patterns provides a high content analysis characterizing the drug and concentration dependent changes (Johnstone et al., 2010; Weiss, 2011). The data are expressed as series means ± SEM. The distributions of the absolute parameters were tested for normality. Using the SPSS (Social Sciences Statistical Software Package), significances of changes induced by the drug exposure were tested by paired t-tests followed by Dunnett's multiple comparison post hoc test with the native activity as the common control and $p < 0.05$ was considered statistically significant. To determine the percentage effective concentrations (EC_{10}, EC_{50}, EC_{90}) sigmoidal standard concentration–response curves – either one or the sum of two, depending on the data – were fitted to the data points using the sum of least squares algorithm of the Solver module in Microsoft Excel (Gramowski et al., 2011).

2.7.3. Pattern recognition and classification analysis of functional compound response patterns

To determine the effects on the electrical activity which were specific for each of the four groups of the drugs in Table 1 these data were further analyzed using methods of pattern recognition. The purpose of pattern recognition is to obtain a reproducible quantitative description of objects or situations which allowed their classification in two or more classes. The recorded time series contain the complex changes in the activity pattern which the administration of a drug causes and leaves behind as a fingerprint. From this a *data record* was extracted, defined as the numerical description of the changes of the activity pattern of one single experimental recording caused by a drug described by the 200 activity features for one concentration and one measurement, which is represented as one data point defined by 200 parameters, which can be envisioned as a data point in a 200-dimensional space. The data records of all treatments of a given drug represent the *drug signature*. This is like the drug's fingerprint as it represents the numerical representation of all changes of the activity patterns caused by the drug. The drug signature comprises the information from all 200 concentration–response curves.

The activity-describing parameters that were used for the drug classification comprise the 30 parameters provided by the software package NeuroExplorer (Nex Technologies, Madison USA) (see e.g. Gramowski et al., 2004), while the remaining 170 are generated by the software package NPWaveX (NeuroProof GmbH, Rostock Germany). These parameters describe different categories of spike train phenomena such as changes in the general activity, the burst structure, network synchronicity and the oscillatory behavior of the activity.

For each concentration, stable activity phases after drug application were selected and the 200 spike train parameters were calculated and normalized by the native activity preceding drug application using NPWaveX® (NeuroProof GmbH, Rostock, Germany) (Parenti et al., 2013; Weiss, 2011). These data records were computed for all 12 compounds and their concentrations yielding a total of 743 data records.

Classifications were performed with artificial neural networks which were trained as multilayer perceptrons with a resilient back-propagation algorithm (Riedmiller and Braun, 1993). All classification and validation steps were performed in a blinded fashion. We used an artificial neural network architecture without hidden layers which is justified because of the biological activity noise. This machine-learning algorithm is implemented in the pattern recognition software platform PatternExpert® (NeuroProof GmbH, Rostock).

2.7.4. Cross validation

To validate the applied approach we performed cross validation where we left out in each of 9 classification rounds 11% of data

records and used the rest for training of the machine learning algorithm. Data records from repeats from one culture or one MEA neurochip were not separated but used only either as learning set or as test set. For testing whether the algorithm can classify the drug correctly into one of the four groups we trained the artificial neural network again as described above.

3. Results

3.1. Effects of repeated treatment on in vitro BBB integrity and drug distribution across the BBB

The *in vitro* BBB model consists of a co-culture of bovine brain capillary endothelial cells (ECs) and neonatal rat glial cells (Fig. 3). The first 12 days of EC differentiation in the presence of glial cells permitted to obtain differentiated brain capillary cells that display most of the BBB characteristics observed *in vivo* (Cecchelli et al., 1999). It was previously reported that these ECs retain their characteristics for two additional weeks (D12–D26) which allow to study repeated drug treatments as demonstrated by (i) the absence of changes in the typical phenotype of confluent bovine brain capillary ECs, (ii) a continued low permeability (Pe) to LY (a non-permeant molecule used as a marker of BBB tightness) and (iii) the similar functional expression of efflux transport systems (such as *p*-glycoprotein (P-gp) and the multi drug resistance protein (MRP) family) from D0 to D14 (Fabulas-da Costa et al., 2013). Therefore, this model has been used to investigate the effects of drug repeated-treatment over a two-week exposure at concentrations relevant to those found in the plasma in humans.

Toxic effects on the BBB were assessed by measuring permeability of the dye LY at several time-points during drug exposure (Fig. 4). The absence of a significant increase of the permeability (Pe) to LY from D0 to D14 in the absence of drug (i.e. control conditions) confirms the restriction of paracellular permeability over time (Fig. 4). A drug was considered to induce a toxic response (impairment of the functionality of the BBB (Fig. 4) when the Pe to LY value of treated cells was significantly higher than the one of control cells (i.e. non-treated cells or cells treated with solvent only at the same time-point) (Culot et al., 2008; Hallier-Vanuxeem et al., 2009). During repeated exposure treatment 10 out of the 12 studied drugs did not show any toxic effects at the BBB level at concentrations relevant to their therapeutic total plasma concentrations in human (Table 1). Indeed, only 15 μM cisplatin and 25 μM propofol were found to exert a toxic effect on the *in vitro* BBB following repeated-exposure treatment (Fig. 4).

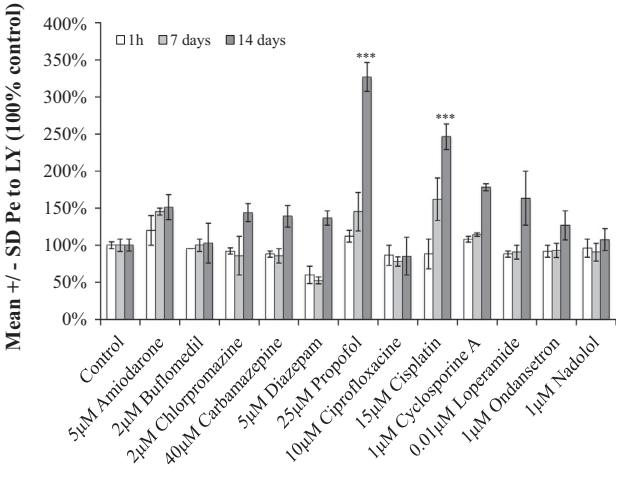


Fig. 4. Effects on the *in vitro* BBB tightness after 1 h of acute exposure or 7 and 14 days of repeated treatment with 12 drugs measured by permeability to LY. Percentage of permeability to LY without treatment is expressed as mean of three experiments ± SD. The 100% control value represent a Pe to LY of 0.23 ± 0.02; 0.33 ± 0.10 and 0.46 ± 0.11 × 10^3 cm min^{-1} after 0, 7 and 14 days respectively. ***-$p < 0.001$ vs. permeability to LY without drug treatment (control) at the same time-point (Tukey post hoc test after a significant ANOVA: $n = 3$ independent EC monolayers/condition).

As further assessed by the *in vitro* BBB permeability studies the 10 tested drugs did not exhibit any BBB toxicity following repeated treatment (Table 2). The Pe values of amiodarone could not be determined due to analytical limitations.

As can be seen in Table 2, all CNS active drugs have a quite high permeability value (i.e. above 2) and the lowest values were obtained for the non-CNS active drugs: nadolol and ciprofloxacin. The slow rate of transport of these two non-CNS active drugs across the *in vitro* BBB is in agreement with their pharmacological targets in peripheral tissues and might explain the absence of neurotoxicity of these drugs as being due to their low ability to cross the BBB and which are thus unlikely to reach the brain parenchyma in significant amounts. However, two other non-CNS active drugs, loperamide and ondansetron, have been found to be highly permeable which indicates that the distribution of these drugs to the brain is not limited due to their ability to cross the brain capillary walls.

The efflux pumps expressed at the BBB are very important in toxicological testing, since they can export potentially harmful substances (Coecke et al., 2006a). Several drugs have been reported to modulate the expression of transporters or efflux pumps at the BBB level, which results in a modification of their CNS distribution. Therefore, the effects of 7 and 14 days of repeated treatment of endothelial cells with the drugs that were not toxic on their rate of distribution across the BBB were evaluated. No significant changes in the distribution rate of the drugs across the BBB were observed following 7 or 14 days of repeated treatments (Fig. 5). In addition, no significant changes in the transcriptional expression of the efflux pumps: ABCB1, ABCG2, ABCC1, ABCC3 and ABCC5 were observed while comparing by qPCR their expression in control ECs to ECs treated with Cyclosporin A, amiodarone, chlorpromazine and diazepam for up to 14 days (partially published in Fabulas-Da Costa et al., 2013).

The BBB permeability is a measurement of the rate of transport of the drug across the BBB, however for neurotoxicity drug evaluation it is not essential to determine how fast a drug crosses the BBB but what concentrations are reached in the brain. Using a recently developed methodology (Culot et al., 2013), the steady-state brain to plasma ratios of the free drugs have been predicted using the *in vitro* BBB model. These ratios have been used together with the free plasma concentration of the drugs to predict the unbound concentrations in brain (Table 3).

Table 2
Evaluation of Pe values (permeability) of the drugs tested using the *in vitro* BBB model.

Drugs	Pe 10^{-3} cm/min	
	Mean ($n = 3$)	SD
Chlorpromazine[a]	3.04	3.52
Buflomedil[a]	6.41	27.45
Ciprofloxacin	0.44	0.09
Carbamazepine[a]	8.35	0.13
Diazepam[a]	4.69	0.16
Cyclosporine A	1.27	1.25
Loperamide	10.94	2.48
Ondansetron	12.51	0.63
Nadolol	0.30	0.04

[a] CNS-active drug.

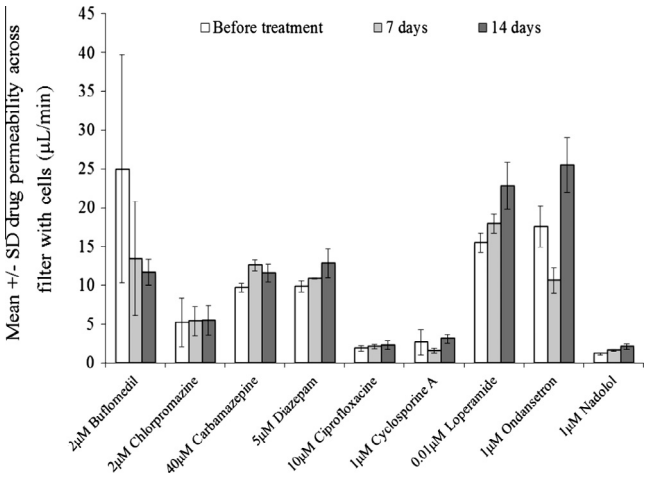


Fig. 5. Effects of 7 or 14 days of repeated treatment of the *in vitro* BBB on the permeability of drugs across the endothelial cell monolayer. Data are expressed as mean of three experiments ± SD of slope of the drug clearance curve across inserts with brain capillary endothelial cells (PSt) assessed before treatment and after 7 or 14 days of repeated exposure to the tested drugs.

3.2. Changes in metabolites in neuronal cell cultures after exposure to drugs

3.2.1. Exposure to amiodarone

3.2.1.1. Cortical network cultures (2D model). Treatment with amiodarone at all three concentrations (3.5 nM, 350 nM, and 1.25 µM) caused down-regulations of 4-aminobutyrate, acetamide, alanine, ß-alanine, choline, creatine, creatine phosphate, glutamate, glutamine, glutathione, glycine, lysine, and o-phosphocholine after 14 days of treatment. Additional down-regulation caused by the low and high concentrations was observed for glutamine after three days, and for glycerol, serine, and threonine after 14 days of exposure. After three days at the high concentration the level of o-phosphocholine was down-regulated whereas ß-alanine was up-regulated. Furthermore, after 14 days of exposure the low concentration induced changes of 2-aminobutyrate, phenylalanine, succinate, and valine and the high concentration of isocitrate, lactate, the secondary messenger precursor myo-inositol, and the neuroactive tyramine (Table 4A, for more details see Table SUPP 1A in Supplementary Material). Glutamate is the key excitatory neurotransmitter in the brain, which when present in excess can cause neuronal cell death through excitotoxicity. It can be converted into glutamine that is mainly present in astrocytes and *vice versa*.

Changes caused by all three concentrations of amiodarone had mostly effects on the amino acid metabolism for a variety of neurotransmitters. There were also a few changes regarding the energy metabolism (e.g. choline, o-phosphocholine, and creatine) including the only up-regulated levels of ß-alanine, which is also an amino acid linked to the neurotransmitter metabolism.

3.2.1.2. Re-aggregating brain cell cultures (3D model). Exposure of re-aggregating brain cell cultures to amiodarone at high concentration (0.625 µM) induced down regulation of the major inhibitory neurotransmitter, 4-aminobutyrate, and the main excitatory neurotransmitter glutamate, affecting also alanine, creatine, lactate, lysine and succinate levels after 14 days of exposure. The up-regulation of alanine, glutamine, phenylalanine and o-phosphocholine was observed already after 3 days of exposure to the low concentration (0.125 µM) (Table 4B, for more details see Table SUPP 1B in Supplementary Material).

3.2.2. Exposure to cylosporine A

3.2.2.1. Cortical network cultures (2D model). After exposure to cyclosporine A, up-regulation of metabolites was induced only by the high concentration (2 µM) at different time points. After three days of treatment changes of malonate and threonine were observed and after 14 days an up-regulation of glycerol and malonate were found. Furthermore, after 14 days of exposure there was a down-regulation of creatine and glycine caused by the high concentration of cyclosporine A. Most down-regulated levels of metabolites were observed only at day 14 of treatment with the low concentration (100 nM). The changes included: 4-aminobutyrate, acetate, aspartate, creatine, glutamate, glutathione, glycine, isocitrate, o-phosphocholine, and threonine (Table 4A). Down-regulation of glutamate, the main excitatory neurotransmitter, could be linked to down-regulation of glutamine that is one of the substrates critical for glutamate synthases.

3.2.2.2. Re-aggregating brain cell cultures (3D model). A Prolonged exposure (14 days) to the high concentration of cyclosporine A (1.0 µM) caused the down-regulation (Table 4B) of the following metabolites: 4-aminobutyrate, acetamide, alanine, choline, creatine, creatine phosphate, glutamate, isoleucine, phenylalanine, succinate, threonine and valine. Up-regulation was observed only for alanine and tyramine after three days of exposure to low concentration of cyclosporine A (0.2 µM) (Table 4B).

Interestingly, in both models down-regulation of the most prominent neurotransmitters, 4-aminobutyrate and glutamate as well as of metabolites linked to energy metabolism was observed.

Table 3
Estimation of the unbound human brain concentrations based on the total plasma concentrations of drugs.

Drugs	Ct,pl (nM)	fu,pl	Cu,pl (nM)	*In vitro* Cu,b/Cu,pl (1 h)	*In vitro* Cu,b/Cu,pl (steady state)[a]	Predicted unbound brain concentration Cu,br (nM)[b]
Chlorpromazine	84–422	0.0220	1.9–9.3	0.17	0.89	**1.7–8.3**
Buflomedil	582–1454	0.3000	174–436	0.45	0.39	**68–170**
Amiodarone	733–2933	0.0002	0.15–0.59	–	–	
Carbamazepine	8465–50,789	0.2400	2032–12,189	0.52	0.58	**1178–7069**
Diazepam	702–7025	0.0100	7.0–70	0.43	0.66	**4.6–46.3**
Propofol	5609–224,379	0.0100	56–2244	–	–	
Ciprofloxacin	7545–12,072	0.7000	5282–8451	0.05	0.09	**475–760**
Cyclosporine A	83–333	0.1000	8.3–33.3	0.02	0.38	**3.1–12.6**
Cisplatin	3333–16,667	0.0250	83–417	–	–	
Loperamide	3–10	0.0590	0.17–0.57	0.17	0.47	**0.08–0.27**
Ondansetron	91–910	0.4680	43–426	0.48	0.58	**25–247**
Nadolol	32–808	0.8000	26–646	0.1	0.07	**1.8–45**

[a] Data obtained following one hour exposure were computed to generate a ratio predicting the distribution at steady-state.
[b] Ct,pl were multiplied by fu,pl to yield Cu,pl. Then Cu,br were estimated by multiplying Cu,pl by the predicted steady-state Cu,br/Cu,pl ratios obtained from the *in vitro* BBB model. For more details refer to Culot et al. (2013).

Table 4A
Changes in metabolites in cortical 2D networks after 3 and 14 days repeated treatment (start at 28 DIV) with the drugs chlorpromazine, diazepam, amiodarone, and cyclosporine A treated with low (L), medium (M) and high (H) concentrations. Data are expressed as fold change per sample pair (treated vs. control).

2D	Drug			
Metabolites	Amiodarone		Cyclosporine A	
	Up	Down	Up	Down
Amiodarone and cyclosporine A				
2-Aminobutyrate		L14* [−2.323]		
4-Aminobutyrate		L14* [−1.567] M14** [−2.500] H14*** [−4.465]		L14* [−2.459]
Acetamide		L14** [−1.945] M14*** [−3.932 H14*** [−61.45]]		
Acetate		M14* [−1.606]		L14** [−1.487]
Alanine		L14** [−5.272] M14* [−4.319] H14* [−4.788]		
Aspartate		H14** [−3.404]		L14* [−2.742]
Choline		L14** [−1.800] M14** [−2.286] H14** [−2.308]		
Citrate		M3** [−1.700] M14*** [−3.400] H14** [−3.180]		
Creatine		L14*** [−4.097] M14*** [−5.429] H14*** [−20.727]		L14*** [−5.123] H14* [−7.536]
Creatine phosphate		L14** [−4.606] M14*** [−6.286] H14*** [−15.278]		L14* [−3.389]
Glutamate		L14*** [−2.152] M14*** [−3.421] H14*** [−9.088]		L14* [2.290]
Glutamine		L3** [−2.466] L14*** [−5.733] M14* [−2.480] H3* [−2.670] H14** [−5.914]		L14* [−2.605]
Glutathione		L14** [−2.400] M14** [−2.965] H14** [−4.552]		L14** [−2.229]
Glycerol		L14** [−2.652] H14** [−2.889]	H3*** [3.395]	
Glycine		L14*** [−3.750] M14*** [−6.632] H14*** [−14.522]		L14** [−6.225] H14* [−7.102]
Isocitrate		H14* [−4.163]		L14** [−3.505]
Lactate		M14* [−2.605] H14* [−3.495]		
Lysine		L14** [−2.326] M14** [−3.620]H14*** [−7.552]		
Malonate		M14* [−2.359]	H3* [2.473] H14** [2.527]	
o-Phosphocholine		L14*** [−2.457] M14*** [−3.264] H3*** [−1.435] H14* [−10.500]		L14** [−3.236]
Serine		L14* [−1.862] H14* [2.320]		
Succinate		L14** [−2.750]		
Threonine		L14* [−2.775] H14* [−4.280]	H3** [2.454]	L14* [−2.477]
Tyramine		H14* [−22.000]		
Valine		L14* [−2.194]		
myo-Inositol		H14* [−2.234]		
β-Alanine	H3* [1.656]	L14** [−2.210] M14* [−2.151] H14* [−3.720]		

(*continued on next page*)

Table 4A (*continued*)

	Drug			
	Chlorpromazine		Diazepam	
	Up	Down	Up	Down
Chlorpromazine and diazepam				
Acetamide		L14** [−1.610] H14*** [−2.442]		L14* [−2.809]
Alanine		L14* [−3.349] H14* [−3.464]		
Citrate		L14* [−1.986]		
Creatine		L14** [−2.567] H14*** [−3.917]		L14** [−4.256] H14** [−3.367]
Creatine phosphate		H14* [−3.824]		L14* [−3.489]
Dimethylamine		L3** [−3.649] L14** [−3.872]		
Glutamate		L14* [−1.646] H14** [−1.709]		
Glutamine		L14** [−2.017]		
Glutathione		L3* [−2.029] L14** [−2.736]		L14* [−2.073]
Glycerol				L14** [−2.235]
Glycine		L14* [−2.405] H14** [−4.280]		
Lysine		L3* [−1.469] L14** [−1.843] H14* [−1.725]		
Malonate				L14* [−2.465]
Methanol				L14* [−1.305]
o-Phosphocholine		L3* [−1.598] L14*** [−2.101] H3* [−1.386] H14*** [−3.655]		L14** [−2.736] H14** [−2.424]
Threonine		L14* [−2.354] H14* [−2.530]		
Tyrosine	L3* [2.682]			
β-Alanine		L14** [−1.841]		

Data are expressed as fold change (in brackets).
L, M, H low, medium or high drug concentration used for exposure (Table 1) 3 or 14 indicate the duration of exposure to the drug (days).
* Significance $p \leqslant 0.05$ (two way ANOVA with Bonferroni post hoc test).
** Significance $p \leqslant 0.01$ (two way ANOVA with Bonferroni post hoc test).
*** Significance $p \leqslant 0.001$ (two way ANOVA with Bonferroni post hoc test).

3.2.3. Exposure to chlorpromazine

3.2.3.1. Cortical network cultures (2D model). After exposure to chlorpromazine (low 10 nM and high 2.5 μM) most down-regulated metabolites levels were observed after 14 days. Changes induced by both concentrations included acetamide, alanine, creatine, glutamate, glycine, lysine, o-phosphocholine, and threonine. The low concentration caused down-regulation of dimethylalanine, glutathione, lysine, an o-phosphocholine and an up-regulation of tyrosine after three days. Tyrosine is, besides its role in protein synthesis, part of signal transduction pathways and it is a main substrate for the synthesis of the neurotransmitters such as dopamine and noradrenalin. After 14 days of exposure the low concentration resulted in a down-regulation of the levels of ß-alanine, citrate, and glutamine. At the high concentration down-regulated changes after three days of treatment were observed for o-phosphocholine and after 14 days for creatine phosphate (Table 4A). An up-regulation of metabolites such as citrate, glutathione, and ß-alanine was observed at both concentrations (Table 4A). There is a resemblance in the observed metabolites changes to those observed after exposure to amiodarone.

3.2.3.2. Re-aggregating brain cell cultures (3D model). There were no significant changes in the metabolite levels found neither over time of treatment nor the concentration after exposure to chlorpromazine of the 3D cultures.

3.2.4. Exposure to diazepam

3.2.4.1. Cortical network cultures (2D model). All changes occurred only after 14 days of treatment and solely down-regulated alterations were observed, mostly for the low concentration. Exposure to both concentrations (low 100 pM and high 10 nM) induced down-regulation of creatine and o-phosphocholine. Changes caused by the low concentration include acetamide, creatine phosphate, glutathione, glycerol, malonate, and methanol (Table 4A). Exposure to diazepam caused predominantly the changes in the metabolites linked to energy metabolism (Table 4A).

3.2.4.2. Re-aggregating brain cell cultures (3D model). Interestingly, in the 3D model exposure to both concentrations (low 0.3 μM and high 1.5 μM) of diazepam induced down-regulation of glutathione but only after 14 days prolonged exposure. The high concentration caused down-regulation of 4-aminobutyrate, choline, lactate, lysine, methanol, and tyramine, the latter was also affected by the low concentration. In contrast, the level of lysine was up-regulated after exposure to the high diazepam concentration after 3 days of exposure (Table 4B).

A comparison of the metabolome changes in two models revealed that there were several metabolites changed in parallel in both, 2D and 3D cultures (see Section 4).

3.3. Protein changes in the neuronal cell culture models after exposure to the selected drugs

Proteins up-regulated by exposure to amiodarone, cyclosporine A, chlorpromazine and diazepam in cortical neuronal network cultures are shown in Table 5A, those down-regulated in Table 5B. Similarly the effects of the same drugs in re-aggregating brain cell

Table 4B
Changes in metabolites in re-aggregating brain cell cultures (3D model) after 3, and 14 days repeated treatment with the drugs chlorpromazine, diazepam, amiodarone, and cyclosporine A treated with low (L), and high (H) concentrations. Data are expressed as fold change per sample pair (treated vs. control).

3D	Drug			
Metabolites	Amiodarone		Cyclosporine A	
	Up	Down	Up	Down
Amiodarone and cyclosporine A				
4-Aminobutyrate		H14* [−1.86]		H14*** [−2.913]
Acetamide				H14*** [−2.441]
Alanine	L3** [1.902]	H14* [−2.100]	L3* [1.378]	H14*** [−2.962]
Choline				H14*** [−1.992]
Creatine		H14* [−1.640]		H14*** [−2.518]
Creatine phosphate				H14*** [−2.239]
Dimethylamine		L14** [−2.969]		
Glutamate		H14* [−1.532]		H14*** [−2.192]
Glutamine	L3* [1.925]			
Isoleucine				H14** [−1.385]
Lactate		H14*** [−1.967]		
Lysine		H14* [−1.573]		
o-Phosphocholine	L3* [1.331]			
Phenylalanine	L3* [1.471]			H14* [−1.528]
Serine				
Succinate		H14* [−1.587]		H14** [−2.254]
Threonine				H14*** [−2.435]
Tyramine			L3* [3.744]	
Valine				H14** [−1.514]

	Drug			
	Chlorpromazine		Diazepam	
	Up	Down	Up	Down
Chlorpromazine and diazepam				
4-Aminobutyrate				H14* [−1.376]
Choline				H14* [−1.418]
Gluthathione				L14** [−1.595]
				H14* [−1.450]
Isocitrate			H3* [1.741]	
Lactate				H14* [−1.567]
Lysine				H14* [−1.305]
Methanol				H14** [−1.342]
Tyramine				L14** [−1.563]
				H14* [−1.442]

Data are expressed as fold change (in brackets).
L, H low or high drug concentration used for exposure (Table 1) 3 or 14 indicate the duration of exposure to the drug (days).
* Significance $p \leqslant 0.05$ (two way ANOVA including Bonferroni post hoc test).
** Significance $p \leqslant 0.01$ (two way ANOVA including Bonferroni post hoc test).
*** Significance $p \leqslant 0.001$ (two way ANOVA including Bonferroni post hoc test).

Table 5
Alterations in intracellular proteins induced by treatment with low (L) or high (H) concentration of amiodarone, cyclosporine A, chlorpromazine or diazepam for 1, 3 or 14 days. Protein names, the corresponding gene names (UniProtKB/Swiss-Prot) and fold changes are listed. Up to five most up- and down-regulated proteins are listed; for the complete list and statistical significances see Supplementary Material Table SUPP 2. Data are expressed as fold change per sample pair (treated vs. control). (A) Proteins up-regulated in the cortical network cultures (2D model). (B) Proteins down-regulated in the cortical network cultures (2D model). (C) Proteins up-regulated in the re-aggregating brain cell cultures (3D model). (D) Proteins down-regulated in the re-aggregating brain cell cultures (3D model).

(A)

Day	Up-regulated			
	Amiodarone		Cyclosporine A	
	Low	High	Low	High
1	DHS, Dhps [1.679] NAC-1, Nacc [1.554] Acyl-CoA synthetase family member 2, mitochondrial, Acsf [1.553] CGG-binding protein, Cggbp1 [1.398]	Leucine-rich repeat-containing protein 66, Lrrc66 [0.012] Protein Traf3ip2, Traf3ip2 [0.012] CCK-AR, Cckar, [0.013] Protein Hy-3, Hydin [0.014] Probable ATP-dependent RNA helicase DDX17, Ddx7 [0.014]	Fz-7, Fzd7 [1.671] MUC-2, Muc2 [3.355] Malignant fibrous histiocytoma-amplified sequence 1 homolog, Mfhas1 [1.718] PL-RP1, Pnliprp1 [1.671] R-PTP-beta, Ptprb [1.661]	Fz-7, Fzd7 [2.017] Iroquois-class homeodomain protein IRX-2, Irx2 [3.600] Abhydrolase domain-containing protein 13, Abhd13 [3.193]

(*continued on next page*)

Table 5 (*continued*)

(A)

Day	Up-regulated			
	Amiodarone		Cyclosporine A	
	Low	High	Low	High
3	mVG5Q, Aggf1 [3.191] Transcription elongation factor A protein 1, Tcea1 [2.685] Protein Dnah1, Dnahc1 [2.079] C1qTNF10, C1ql2 [2.861] Protein Aadacl2, Aadacl2 [2.551]	mVG5Q, Aggf1 [0.011] Transcription elongation factor A protein 1, Tcea1 [0.011] Protein Dnah1, Dnahc1 [0.013] Protein Aadacl2, Aadacl2 [0.013] CCK-AR, Cckar [0.013]	Canalicular multispecific organic anion transporter 1, Abcc2 [5.047] Thimet oligopeptidase, Thop1 [2.928] Puromycin-sensitive aminopeptidase, Npepps [2.658] TRMT1-like protein, Trmt1l [2.058]	Cat eye syndrome critical region protein 5 homolog, Cecr5 [2.239] Otopetrin-2, Otop2 [2.175] Telomerase Cajal body protein 1, Wrap53 [2.091]
14	Vasculin-like protein 1, Gpbp1l1 [2.828] Olfactory receptor 584, Olfr584 [2.452] UBX domain-containing protein 7, Ubxn7 [2.369] ADAM-TS 18, Asamts18 [2.296] Dual specificity protein phosphatase 26, Dusp26 [2.285]	Serine-protein kinase ATM, Atm [0.012] PHLP, Pdcl [0.015] Coiled-coil domain-containing protein 80, Ccdc80 [0.016] LPA-2, Lpar2 [0.017]	DNA polymerase alpha catalytic subunit, Pola1 [2.364] MtMetRS, Mars2 [2.286] Kinesin-like protein KIF11, Kif11 [2.258] Transmembrane protein 147, Tmem147 [2.159] MUC-2, Muc2 [2.141]	mH2a2, H2afy2 [2.791] Protein Wdr63, Wdr63 [2.487] Exocyst complex component 3-like protein, Exco3l1 [2.308] H2a/x, H2afx [1.971] Olfactory receptor 985, Olffr985 [1.865]

	Up-regulated			
	Chlorpromazine		Diazepam	
	Low	High	Low	High
1	mROR1, Ror1 [2.306] Short-chain dehydrogenase/reductase family 16C member 6, Sdr16c6 [2.078]	Proteasome activator complex subnit 4, Psme4 [1.777] Creatine kinase M-type, Ckm [1.495]	RdCVF2, Nxnl2 [2.012] Protein Magee2, Magee2 [1.883] Int5, Ints5 [1.756] mSIM, Sim2 [1.723]	AKAP-3, Akap3 [1.993] DNA replication licensing factor MCM2, Mcm2 [1.693] Fibillin-2, Fbn2 [1.685] CA-XV, Ca15 [1.603] Protein Vmn2r24, Vmn2r24 [1.569]
3	Synaptotagmin-16, Syt16 [2.649] Olfactory receptor 1167, Olfr 1167 [2.338]	Synaptotagmin-16, Syt16 [3.689] Olfactory receptor 1167, Olfr 1167 [4.223] Protein Gpr111, Gpr111 [3.249] mPAST2, Ehd4 [2.712] LIM homeobox transcription factor 1-beta, Lmx1b [2.697]	Protein Lct, Lct [1.945] Beta-actin-like protein 2, Actbl2 [1.876] DBH-like monooxy-genase protein 1, Moxd1 [1.845] NF-M, Nefm [1.506]	Interferon-inducible GTPase 1, ligp1 [1.767] Histone H3.1, Hist1h3a [1.583] Protein Magee2, Magee2 [1.420]
14	GLAST-1, Slc1a3 [1.986] Keratin, type I cytoskeletal 10, Krt10 [2.558]	GLAST-1, Slc1a3 [1.798] Neurexin-3, Nrxn3 [1.990] Fxn, Fxn [1.980] Cathepsin Z, Ctsz [1.856] Protein Edem2, Edem2 [1.849]	Synaptojanin-1, Synj1 [3.05] Protein Lct, Lct [2.689] Tripartite motif-containing protein 44, Trim44 [2.166] Myotrophin, Mtpn [2.053] Protein NDRG1, Ndrg1 [1.865]	M-phase inducer phosphatase 3, Cdc25c [3.111] GST 1-1, Gstm1 [3.005] Armadillo repeat-containing X-linked protein 3, Armcx3 [2.557] Beta-actin-like protein 2, Actbl2 [2.161] mSIM, Sim2 [1.925]

(B)

Day	Down-regulated			
	Amiodarone		Cyclosporine A	
	Low	High	Low	High
1	Homeobox protein Meis1, Meis [0.346] NCoA-2, Ncoa2 [0.131] Placenta-specific protein 1, Plac1 [0.273] Olfactory receptor, Olfr640 [0.349]	Homeobox protein Meis1, Meis [0.519] Fibrillin-2, Fbn2 [0.335] Protein Zfp236, Zfp236 [0.433] TIF1-beta, Trim28 [0.552]	Kinesin-like protein KIF3B, Kif3b [0.247] Protein Abca12, Abac12 [0.463] Skint-8, Skint8 [0.477] Synaptojanin-1, Synj1 [0.583]	Olfactory receptor, Olfr1100 [0.300] Olfactory receptor, Olfr676 [0.267] SEL-OB, Svep1 [0.273] HD10, Hdac1 [0.275] Olfactory receptor, Olfr202 [0.203]
3	Neurexin-3, Nrxn3 [0.049] PAX3/7BP, Gcfc1 [0.268] Zinc finger protein GLI2, Gli2 [0.280] Nuclear pore complex protein Nup155, Nup155 [0.403] Autophagy-related protein 2 homolog B, Atg2b [0.478]	Neurexin-3, Nrxn3 [0.119] LRP-2, Lrp2 [0.328] Protein FAM13B, Fam13b [0.507] Ankyrin repeat domain-containing protein 49, Ankrd49 [0.569] Protein Morn1, Morn1 [0.609]	RNA polymerase I subunit A49, Polr1e [0.394] PP, Ppy [0.455]GC-1, Slc25a22 [0.471] ER membrane protein complex subunit 2, Emc2 [0.566]	SEL-OB, Svep1 [0.397] DNA replication licensing factor MCM6, Mcm6 [0.344] Puromycin-sensitive aminopeptidase, Npepps [0.370] BAL, Cel [0.540]
14	Slc22a3, Slc22a3 [0.013] cPLA2-zeta, Pla2g4f [0.013] Olfactory receptor, Olfr393 [0.044]	Slc22a3, Slc22a3 [0.121] Claudin-15, Cldn15 [0.069] MOB kinase activator 1B, Mob1b [0.071] Nuclear pore complex protein Nup155, Nup155 [0.146] E3 ubiquitin-protein ligase Hakai, Cb1l1 [0.378]	MAP-6, Map6 [0.407] mTaar2, Taar2 [0.511] H2a/x, H2afx [0.562] CGG-binding protein 1, Cggbp1 [0.575] SLIT and NTRK-like protein 5, Slitrk5 [0.576]	MAP-6, Map6 [0.503] mTaar2, Taar2 [0.427] Uncharacterized protein KIAA1671, Kiaa1671 [0.527] BGnT-7, B3gnt7 [0.540]

Table 5 (*continued*)

	Down-regulated			
	Chlorpromazine		Diazepam	
	Low	High	Low	High
1	IRS-4, Irs4 [0.325] Protein Plekha5, Plekha [0.332] Cleavage stimulation factor subunit 2, Cstf2 [0.471] C1qTNF10, C1q12 [0.601] Collagen alpha-1(XXVII) chain, Col27a1 [0.693]	IRS-4, Irs4 [0.494] Platelet-activating factor acetylhydrolase IB subunit beta, Pafahl1b2 [0.607] NEC 1, Pcsk1 [0.660] Protein FAM13B, Fam13b [0.667]	Ca-XV, Ca15 [0.55] Proteasome subunit beta type-10, Psmb [0.562] tRNA (cytosine (38)-C(5))-methyltransferase, Trdmt1 [0.609]	Neuronal PAS4, Npas4 [0.484] G alpha-15, Gna15 [0.539] Contactin-3, Cntn3 [0.658]
3		Exocyst complex component 4, Exoc4 [0.176] Protein Taf15, Tafl5 [0.219] Progressive ankylosis protein, Ankh, [0.295] Thiosulfate sulfurtransferase/rhodanese-like domain-containing protein 3, Tstd3 [0.299]	Microsomal GST-3, Mgst3 [0.605] Homeobox protein Meis1, Meis1 [0.636] UBX domain-containing protein 7, Ubxn7 [0.684]	MAP-6, Map6 [0.457] Homeobox protein Meis1, Meis1 [0.602] abLIM-3, Ablim3 [0.628] Heparan sulfate 2-O-sulfotransferase 1, Hs2st1 [0.638] Tripartite motif-containing protein 44, Trim44 [0.905]
14	Collagen alpha-1(XVI) chain, Col16a1 [0.588] snRNP-N, Snrpn [0.561]	Collagen alpha-1(XVI) chain, Col16a1 [0.515] CNIH-2, Cnih2 [0.488] Protein Olfr655, Olfr655 [0.505] Spermatid-specific linker histone H1-like protein, Hils1 [0.591] Protein Zim1, Zim1 [0.599]	Protein Gm1527, Gm1527 [0.549] Testis-expressed sequence 12 protein, Tex12 [0.558] SNAP-25, Snap25 [0.565] Integral membrane protein 2C, Itm2c [0.587]	Int5, Ints5 [0.263] Integral membrane protein 2C, Itm2c [0.434] Testis-expressed sequence 12 protein, Tex12 [0.601] SNAP-25, Snap25 [0.666]

(C)

Day	Up-regulated			
	Amiodarone		Cyclosporine A	
	Low	High	Low	High
1	Synaptogamin-10, GW7_10229 [2.493] Protein kinase C iota type, GW7_20227 [2.530]	Synaptogamin-10, GW7_10229 [2.507] Histone H2A, H2afx [6.051]	Glutaminyl-tRNA synthetase, Qars [10.825] U1 snRNP C, Snrpc [4.126]	
3	Peroxiredoxin-6, GW7_21572 [3.282] Protein Fam9b, LOC100360496 [2.355] Serine-threonine-protein kinase Nek1, GW7_03032 [2.595] Zinc finger protein 638, GW7_03453 [2.369]	Peroxiredoxin-6, GW7_21572 [2.571] Protein Fam9b, LOC100360496 [2.681] Protein Ccdc111, Ccdc111 [2.489] Tubulin alpha-8 chain, GW7_16361 [2.391]	Cytochrome b-c1 complex 1 subunit Rieske, mitochondrial, Uqcrfs1 [2.046] Calcium-transporting ATPase, GW7_12839 [0.1.875] Ribosome biogenesis protein NSA2-like protein, GW7_16230 [2.407]	Protein Hirip3, Hirip3 [1.918]
14		Peroxiredoxin-2, GW7_16090 [2.977]	Macrophage migration inhibitory factor, Mif [2.975]	Tumor necrosis factor, alpha-induced protein 2, GW7_18863 [2.995]

	Up-regulated			
	Chlorpromazine		Diazepam	
	Low	High	Low	High
1	Nuclear pore complex protein Nup214, G5AT56 [2.744] Protein Nubp, D3ZFQ3 [2.317] Synphilin-1, GW7_06799 [3.182]	Lysophos-phatidylcholine acyltransferase 4	Dihydropteridine reductase, GW7_16632 [1.772] Lactoylglutathione lyase, GW7_08996 [3.627]	
3	Arylsulfatase J, GW7_15968 [2.689]	Chemokine (C–C motif) receptor 7, Ccr7 [2.603] Heterochromatin protein 1-binding protein 3, GW7_01848 [2.393]	Epsilon 1 globin, Hbe1 [1.670] Olfactory receptor, Olfr125 [1.880] Dedicator of cytokinesis protein 5, GW7_07635 [2.694] Protein Npat, Napt [1.655]	Epsilon 1 globin, Hbe1 [1.772] Olfactory receptor, Olfr125 [2.129] Histone deacetylase 1, GW7_10470 [3.901]
14	2-oxoglutarate dehydrogenase E1 component-like, mitochondrial, GW7_10398 [8.747]	Dermcidin, Dcd [3.404] Keratin, type I cytoskeletal 10, GW7_15073 [4.973]	Lysophospholipid acyltransferase 5, Lpact3 [2.029] Protein LOC100909742, RGD1566085 [1.774] Protein RGD1560175, RGD1560175 [2.115]	

(*continued on next page*)

Table 5 (*continued*)

(D)

Day	Down-regulated			
	Amiodarone		Cyclosporine A	
	Low	High	Low	High
1	ORM1-like protein 3, Ormdl3 [0.446] NAD-dependent deacetylase sirtuin-2, GW7_16704 [0.147]	Protein RGD1559970, RGD1559970 [0.418]		Acid ceramidase, Asah1 [0.403]
3	Protein Cenpf, Cenpf [0.370] Protein Rictor, Rictor [0.383]		HD8, GW7_09216 [0.276] Histone H2A, H2afy2 [0.530]	HD8, GW7_09216 [0.355] Serine/threonine-protein kinase 4, GW7_18343 [0.508]
14		Ac1-130, LOC301444 [0.311] EGF receptor substrate 15-like 1, GW7_08355 [0.240] Protein Slirp, Slirp [0.033] RE1-silencing transcription factor, Rest [0.388] Splicing factor, arginine–serine-rich17A, GW7_13383 [0.153]		14-3-3 protein eta, Ywhah [0.406]

	Down-regulated			
	Chlorpromazine		Diazepam	
	Low	High	Low	High
1	Protein Aqp12a, D4A9T6 [0.248]	Protein Aqp12a, D4A9T6 [0.302] Condensin-2 complex subunit G, GW7_10628 [0.450] GRAM domain-containing protein 1A, GW7_18387 [0.278]	Clathrin light chain B, Cltb [0.404]	
3	ATPase subunit F6, Atp5j [0.365] GAPDH, N/A [0.401] Dynein heavy chain 3, axonemal, GW7_04731 [0.467]	ATPase subunit F6, Atp5j [0.320] GAPDH, N/A [0.316] 40S ribosomal protein S24, GW7_05671 [0.329] MSR, Mtrr [0.390] Protein deltex-1, GW7_10150 [0.384]		Citrate synthase, GW7_15757 [0.158] NADH dehydrogenase [ubiquinone] 1 beta subcomplex subunit 6, GW7_13110 [0.449] Olfactory receptor, GW7_16219 [0.392] Protein Dmrtb1, Dmrtb1 [0.634]
14	Similar to receptor expression enhancing protein 2, LOC682105 [0.384]		Lactoylglutathione lyase, GW7_08996 [0.376]	Lactoylglutathione lyase, GW7_08996 [0.216] Cytochrome c oxidase subunit 8B, mitochondria, Cox8b [0.346] Sushi, nidogen and EGF-like domain-containing protein 1, GW7_11065 [0.340] Protein Ablim3, Ablim3 [0.349] Protein RGD1305184, RGD1305184 [0.426]

cultures (3D model) are shown in Table 5C and D. The total number of significantly ($p \leqslant 0.05$) enriched or depleted proteins varied depending on the drug. For the 2D neuronal model 211 proteins were detected for amiodarone over all three time points and both concentrations, 110 for cyclosporine A, 52 proteins for chlorpromazine, and 102 for diazepam. For the 3D model the following numbers of significantly altered proteins were detected for amiodarone 112, for cyclosporine A 36, for chlorpromazine 32, and for diazepam 125. Only those proteins detected in all three biological repeats were further taken into consideration. At each individual time point and concentration only a subfraction of those proteins were changed significantly, out of which the top up and down-regulated proteins are represented in Table 5 including their fold-change and relative abundance. An additional table with all proteins analyzed for the 2D and the 3D model is given in Table SUPP 2 in Supplementary Material. The treatment with the same drug at low or high concentration showed some similarities but the majority of altered proteins were different. Also treatment for 1, 3 or 14 days caused mainly deregulation of different proteins.

When the up- and down-regulation patterns of the four drugs were compared the changes in the two neuronal culture systems (Table 5A and B vs. C and D) showed low similarity. This indicates that the three drugs considered to be neurotoxic (amiodarone, cyclosporine A, chlorpromazine) act through completely different mechanisms and show no common pathways of toxicity with diazepam which was grouped as non-neurotoxic.

3.3.1. Exposure to amiodarone

3.3.1.1. Cortical network cultures (2D model). The function of the majority of the observed up- and down-regulated proteins is not specific for neuronal cells. There are only a few up regulated neuron-specific proteins observed after exposure to the low concentration, such as the neuronal corepressor NAC-1, Acyl-CoA synthetase family member 2, CGG-binding protein (mental retardation related), ADAM-TS 18, and the MAPK inactivator "dual specificity protein phosphatase 26". The neuron specific proteins similarly down-regulated after 3 and 14 days were the neuronal cell adhesion protein, neurexin-3 and the transmitter regulator Slc22A3.

3.3.1.2. Re-aggregating brain cell cultures (3D model). Interestingly, after exposure of 3D neuronal culture to amiodarone, among other proteins (serine–threonine-protein kinase Nek1, histone H2A, Zinc finger protein 638 peroxiredoxin-6, protein Ccdc111, protein Fam9b, tubulin alpha-8 chain, peroxiredoxin-2) up-regulation of synaptogamin-10 was observed by both concentrations (low and high) already after 1 day of exposure (Table 5C). Synaptogamins

are presynaptic proteins involved in vesicle exocytosis, a process critical for the synaptic neurotransmission and specific for neuronal function.

3.3.2. Exposure to cyclosporine A

3.3.2.1. Cortical network cultures (2D model). After exposure to cyclosporine A changes in a number of proteins were observed (Table 5A and B) some of which have special relevance for neuronal function, namely the up-regulated thimet oligopeptidase (degrading APP) or the down-regulated proteins synaptojanin-1 (vesicle binding and regulating) (Cremona et al., 1999), the modulator of transmission GC-1, the glutamate carrier CGG-binding protein 1, the ABC transporter Abca12, the kinesin-like motor protein KIF3B, or the neurite outgrowth suppressor SLIT and NTRK-5. These changes were seen almost entirely at the low concentration, except for MAP-6, which was down-regulated by both concentrations.

3.3.2.2. Re-aggregating brain cell cultures (3D model). The exposure of 3D re-aggregating brain cells to high concentration of cyclosporine A induced down-regulation of acid ceramidase, histone deacetylase 8, serine/threonine-protein kinase 4, tumor necrosis factor, alpha-induced protein 2, 14-3-3 protein eta while the lower concentration affected levels of histone deacetylase 8 and histone H2A (Table 5D). However, exposure to low cyclosporine concentration caused up-regulation of glutaminyl-tRNA synthetase, U1 small nuclear ribonucleoprotein C, Cytochrome b-c1 complex 1subunit Rieske, mitochondrial, plasma membrane calcium-transporting ATPase 4, ribosome biogenesis protein NSA2-like protein and macrophage migration inhibitory factor (Table 5C). The function of these down- and up-regulated proteins is not specific for neuronal cells, suggesting that the observed changes could be linked to cyclosporine A induced cytotoxicity.

3.3.3. Exposure to chlorpromazine

3.3.3.1. Cortical network cultures (2D model). The proteins altered after the exposure to chlorpromazine (low 10 nM and high 2.5 μM) with potential CNS-relevance were synaptotagmin-16, olfactory receptor 1167, creatine kinase, neurexin-3, and GLAST-1, the excitatory amino acid transporter responsible for synaptic glutamate reuptake (Table 5A). Synaptotagmins are the Ca^{2+} sensors needed for all exocytosis of neurotransmitters and hormones. Synaptogamin-10 triggers in certain neurons exocytosis of insulin-like growth factor 1 (IGF-), important during organogenesis in the CNS (Cao et al., 2011). CNS-related proteins which were down-regulated included neuroendocrine convertase 1 (NEC 1) and the AMPA glutamate receptor regulator CNIH-2 (Table 5B).

3.3.3.2. Re-aggregating brain cell cultures (3D model). Exposure of 3D neuronal cultures to chlorpromazine deregulated mainly the expression of proteins involved in general cell function (Table 5C and D). However, two proteins have been identified that play an important role in specific neuronal functions namely dynein heavy chain 3 (down-regulated by low concentration of chlorpromazine after 3 days of exposure) and synphilin-1 (up-regulated after 1 day of treatment with low concentration). Dynein carries organelles, vesicles and possibly microtubule fragments along the axons of neurons toward the cell body in a process called retrograde axoplasmic transport (Waterman-Storer et al., 1997) and synphilin-1 is widely expressed in brain and accumulates in the neuropil during development. Synphilin-1A may contribute to neuronal degeneration in α-synucleinopathies. Overexpression of synphilin-1A in neurons results in striking cellular toxicity and it is present in Lewy bodies of patients with Parkinson's disease (Eyal et al., 2006).

3.3.4. Exposure to diazepam

3.3.4.1. Cortical network cultures (2D model). After exposure to diazepam at both concentrations an up-regulation of proteins potentially relevant to CNS functions such as, beta-actin-like protein 2, dopamine-beta-hydroxylase-like monooxygenase, neurofilament medium chain (NF-M), Synaptojanin-1 (Table 5A) was observed. Down-regulated were SNAP-25, neuronal PAS4 (responsible for a degenerative CNS disorder) and microtubule-stabilizing MAP-6 (Table 5B). The neuronal transcription factor mSIM was up-regulated at all time points, while mSIM and the synaptosomal associated protein 25 (SNAP 25) and integral membrane protein 2C, neuronal PAS 4 and the microtubule stabilizer MAP-6 were down-regulated (Table 5B). SNAP-25 is a membrane-bound protein necessary for presynaptic release of neurotransmitters and inhibits P/Q- and L-type voltage-gated calcium channels located presynaptically (Hodel, 1998). It interacts with synaptotagmin in transmitter release (Chapman, 2002).

3.3.4.2. Re-aggregating brain cell cultures (3D model). In the 3D model diazepam deregulated a few proteins involved in general cell function and one olfactory receptor protein was up-regulated by both concentrations of diazepam after 3 days of exposure (Table 5C and D).

A comparison of the models was performed by correlating the proteome changes in the 2D with those in the 3D cultures. It revealed that there are few proteins which are changed in parallel in both models. Either the slopes of regression lines or the significances or both were very low, indicating that the two models are considerably different (see Supplementary Material Fig. SUPP 1). Therefore, a principal Component Analysis (PCA) was not performed.

3.4. Electrical activity of neuronal networks as an endpoint for prediction of neurotoxicity

Complementary to the metabolomics and proteomics analysis drug-induced neurotoxicity has been evaluated by a functional test based on measurement of the changes of neuronal electrical activity patterns. To develop an experimental design for an optimal assessment and a clear definition of neurotoxicity based on the evaluation of neuronal electrical activity, 12 drugs belonging to 4 groups (Table 1) were selected as reference. The changes of neuronal network activity induced by acute exposure to these drugs were analyzed and quantified by multivariate data analysis, calculating 200 activity features from the activity pattern data records. As an example of the 200 concentration–response curves those for one activity feature, namely *spike rate* are shown in Fig. 6. The concentration-dependence of all 200 activity features yields a characteristic drug signature for each drug.

On the basis of drug signatures derived from acute concentration–response curves an artificial network was trained and the specific changes and common features for the three compounds in each class which allowed to group the drugs into the four classes.

There are clear differences between the drugs' responses (Fig. 6) such as different curve shapes, some being biphasic and present different EC_{50} values. A second example out of the 200 such curves, *burst duration*, is shown in the Supplementary Material Fig. SUPP 2 to demonstrate that the concentration-dependent behaviors of the parameters differ considerably from each other. A comparison of the effects of the drugs on the different parameters, such as for example Fig. 6 and Fig. SUPP 2, demonstrates that they are all different to a larger or lesser extent.

In Fig. 6 the vertical lines show for comparison the cytotoxicity of the high concentrations (up to about 10–20% cytotoxicity after 1 day exposure) as estimated by released LDH measurements. It

can be seen that for many drugs the parameter depicted shows significant pattern changes at concentrations still lower than those causing cytotoxic effects.

To estimate the quality of the classification system a cross validation test was performed (see Section 2). Table 6 shows that using the data from the low concentration experiments the drugs of classes I to II were correctly classified as seen by the highest scores of correct assignments for one class (highest percentages in dark shading). Class IV being non-neuroactive and non-neurotoxic showed weaker effects and was therefore correctly assigned in only 22% and often confused with class III compounds. Interestingly, when using the data records from the high concentration experiments all drugs were classified correctly.

4. Discussion

Testing of many compounds with a desired pharmacological effect for toxicity represents one of the bottlenecks in drug development since it is extremely complex, time consuming, requires large numbers of animal experiments and might deliver data not necessarily relevant to human physiology (Fung et al., 2001; Schuster et al., 2005). Recently, the scientific and regulatory community is becoming increasingly aware of the limitations of the current safety testing paradigm that is mainly based on *in vivo* studies (Judson et al., 2013; Leist et al., 2014; Rovida et al., 2015). This topic is worldwide discussed during the last years leading to the paradigm shift in toxicology, from the animal apical endpoints evaluation to more mechanism-based predictive toxicology. Therefore, there is a need for more predictive and efficient methods that would detect also neurotoxic drug or chemical effects and give insight into mechanisms and pathways of neurotoxicity (Bal-Price et al., 2012; Smirnova et al., 2014).

Very high attrition rate (Kola and Landis, 2004) and too few compounds to begin with are the reason for inefficient drug development for neurodegenerative diseases, including Alzheimer's disease (Cummings et al., 2014). Agid et al. (2007) point out the need for a multidisciplinary approach based on combining human

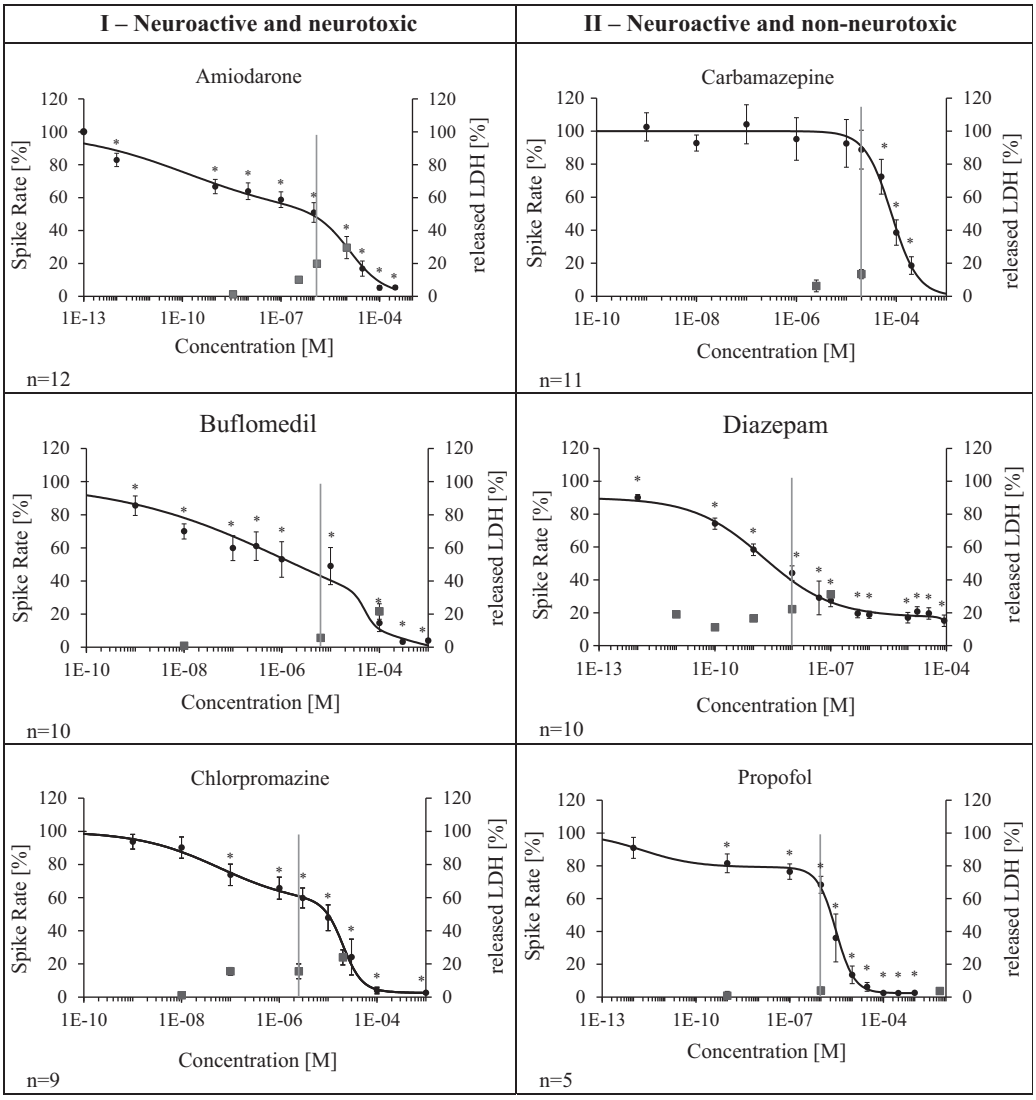


Fig. 6. Concentration–response curves for the activity parameter "spike rate" (series mean ± SEM) measured after acute exposure to the 12 drugs grouped into four classes. Independent cytotoxicity measurements for the low concentration after 1 day exposure (squares, released LDH assay, % of Triton X100 lysis control, mean ± SD) are included to show that alterations of the electrical activity occurred frequently at non-cytotoxic concentrations. For comparison the high concentration is indicated by a vertical line. Significances according the paired *t*-test and Dunnett's multiple comparison posthoc test are given with a *p*-value of at least $^{*}p < 0.05$. From equations fitted to the data the following EC_{50} values were obtained for the drugs: amiodarone: 12.8 μM, buflomedil: 12 μM, chlorpromazine: 2.03 μM, carbamazepine: 0.80 μM, diazepam: 0.165 nM, propofol: 3 μM; cisplatin: 2 μM, cyclosporine A: 69.9 μM, ciprofloxacin: 22.4 μM, loperamide: 6.12 μM, nadolol: 313 μM, ondansetron: 12.3 μM.

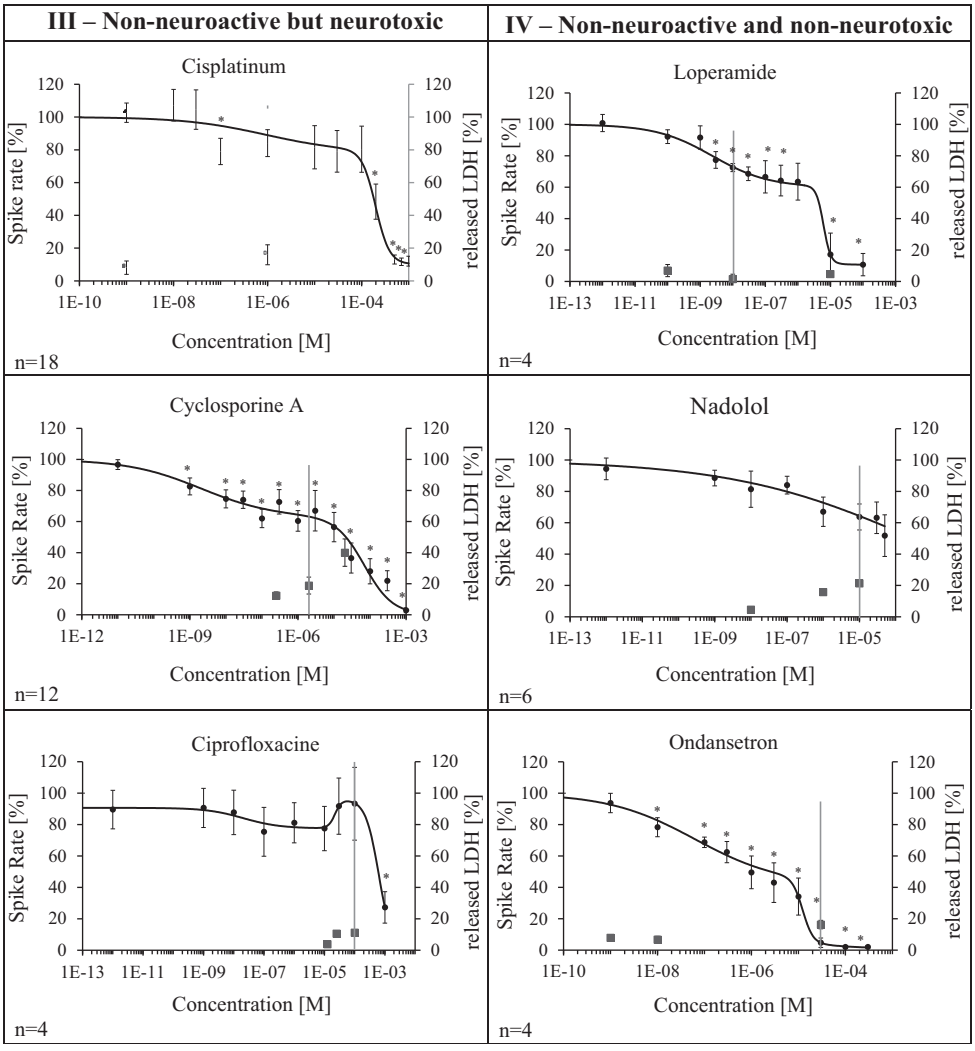


Fig. 6 (*continued*)

Table 6
Cross validation of the data records of the four compound groups against each other and number of data records included in the classification.

Low concentration

Class	I	II	III	IV	Data records
I: neuroactive/ neurotoxic	44	24	18	14	118
II: neuroactive/ non-neurotoxic	20	47	23	10	116
III: non-neuroactive/neurotoxic	14	25	45	16	157
IV: non-neuroactive/non-neurotoxic	9	24	45	22	55

High concentration

Class	I	II	III	IV	Data records
I: neuroactive/ neurotoxic	62	17	13	8	53
II: neuroactive/ non-neurotoxic	23	40	29	8	87
III: non-neuroactive/neurotoxic	9	26	55	10	120
IV: non-neuroactive/non-neurotoxic	19	30	16	35	37

correct self recognition

false self recognition

Data record: the numerical description of the changes of the activity pattern of one single experimental recording caused by a drug described by the 200 activity features for one concentration and one measurement. Numbers indicate % correctly identified data records. The highest score in each line indicates the group for which the data records of a given drug were classified by maximum similarity.

Table 7
Metabolites down-regulated in both the 2D and the 3D models.

Amiodarone	Cyclosporine A	Diazepam
4-Aminobutyrate	**Creatine**	Glutathione
Alanine	4-Aminobutyrate	Methanol
Creatine	Creatine phosphate	
Glutamate	Glutamate	
Lactate	Threonine	
Lysine		
Succinate		

Bold: metabolites down-regulated in the 2D and 3D models at the high concentration after 14 days, non-bold: down-regulated at the same time points but different concentrations.

exposure information with signaling toxicity pathways and phenotypic physiology measurements for successful drug discovery.

In the present study, we aimed to develop an improved *in vitro* approach for neurotoxicity testing by combining *in vitro* BBB studies with neuronal functional evaluation (electrical activity measurements) and OMICs analysis in order to provide some mechanistic insight into drug-induced toxicity that could be further elaborated using the adverse outcome pathway (AOP) concept. Recently the AOP concept has been proposed as a tool for systematic evaluation of molecular understanding of pathways of toxicity, including neurotoxicity (Bal-Price et al., 2015a) for human risk assessment (Landesmann et al., 2013).

Building an integrated testing strategy (ITS) based on OMICs analyses (transcriptomics, metabolomics and proteomics) combined with electrical activity profiling has the potential to considerably advance our understanding of drug-induced cellular perturbations of physiological pathways that once sufficiently perturbed become toxicity pathways. The proposed ITS includes an *in vitro* BBB model that allows to detect toxic effects at the BBB level followed by the application of the complementary, well characterized *in vitro* neuronal/glial mixed cell cultures such as the 3D model of rat primary re-aggregating brain cell and the 2D murine neuronal network of cortical neurons. The applied endpoints permitted to study a broad range of possible cellular targets of drug-induced toxicity, leading to the identification of putative neurotoxicity biomarkers.

4.1. Blood brain barrier (BBB)

The knowledge of drug distribution in the brain, which is strictly regulated by the function of the BBB, is essential for drug development. Neuropharmaceuticals must attain sufficient concentration in the brain to elicit the desired pharmacological effect whereas for drugs that have pharmacological targets in peripheral tissues a low distribution in the brain parenchyma could prevent any CNS-side effects. The evaluation of drug-induced toxicity at the BBB is equally important as a dysfunctional BBB as it may cause unwanted, indirect neurotoxicity by disturbing the homeostasis of the brain and increasing the amount of compound penetrating through the BBB. For this reason an *in vitro* blood brain barrier model that consists of the co-culture of bovine endothelial cells and primary culture of rat astrocytes was established and functionally characterized to determine acute and repeated treatment toxicity. The co-culture with glial cells is required to keep the barrier properties of the endothelial cells over time. The permeability to drugs was measured without the presence of glial cells during the 1 h of the transport experiment, whereas the *in vitro* experiments to determine the unbound brain/plasma ratios required the glial cells which are used to mimick the brain tissue binding. The role of astrocytes in the induction/maintenance of the BBB function has been discussed previously in the work of Fabulas-Da Costa et al., 2013 where also the possibility to replace the coculture of glial cells with glial cell-conditioned medium has been discussed.

The direct toxicity induced by a drug to the endothelial cells of the BBB is assessed by their ability to maintain a tight and functional barrier between the two compartments. Therefore, the BBB permeability to the fluorescent marker Lucifer Yellow is used to evaluate the toxicity. This hydrophilic compound should not permeate the BBB so that any significant increase in its permeability across the endothelial cell monolayer reveals an alteration in the functionality of the barrier. We tend to consider this endpoint as much more reliable than any non-functional marker. BBB function can also be evaluated by the measurements of trans-epithelial electrical resistance (TEER) (Boveri et al., 2006).

The rates of transport of the drugs across the BBB were studied and the permeability values obtained from the *in vitro* BBB model were comparable with *in vivo* data. All studied CNS active drugs were found to have high BBB permeability (i.e. above 2×10^{-3} -cm/min) and the lowest BBB permeabilities were found for the peripherally acting drugs.

To our knowledge, this is the first time an *in vitro* BBB model has been adapted for long term repeated-exposure treatment. Ten out of the 12 studied drugs at the clinically relevant concentrations did not show any toxic effects at the BBB level. Only 15 μM cisplatin and 25 μM propofol were found to exert a toxic effect following repeated treatment. Propofol is used on an acute basis for the induction and maintenance of general anesthesia and chronically for long-term sedation of mechanically ventilated patients. There is no published evidence to suggest that propofol is toxic to the BBB. Cisplatin is an anticancer drug that is usually administered intravenously as a short-term infusion. On the basis of *in vivo* studies in rats and rabbits, it has been suggested that the neurological adverse reactions reported for cisplatin in humans could be associated with BBB disruption (Namikawa et al., 2000; Sugimoto et al., 1995). The absence of toxicity for 10 of the tested drugs was not expected based on *in vivo* studies. Furthermore, exposure of the *in vitro* BBB model to repeated treatments of cisplatin and colchicine, two drugs associated with drug-induced neuropathy in humans (positive controls), but with limited distribution across the BBB, were found toxic in agreement with similar *in vivo* findings (Fabulas-Da Costa et al., 2013).

In this study it has been proved that *in vitro* BBB model can be applied for both acute and chronic exposure and it is important to evaluate both time points as in some cases the BBB permeability of the same drug after acute treatment differs from that after chronic exposure as it was found in the case of cisplatin and propofol.

Furthermore, the finding that two non-CNS active drugs, loperamide and ondansetron, have been found to be highly permeable through BBB indicates that the distribution of these drugs to the brain could be high. Loperamide is a μ-opioid agonist and therefore it shows effects in the MEA neurochip assay. This seems to contradict the findings in the BBB study and in patients. But this can be explained by its active export by the p-glycoprotein transporters (Montesinos et al., 2014). Indeed, as illustrated in Table 3, the concentration of loperamide predicted to reach the CNS is quite low. This opoid derivative, used as an anti-diarrheal agent, is poorly adsorbed which explains the low concentration found in plasma after oral administration. In animals, experiments with P-gp knockout showed a 17-fold higher brain concentration of the loperamide metabolite (desmethyl-loperamide) (Wanek et al., 2013). This correlates with our finding of electrophysiological changes in the absence of a BBB and it may have affected the cross validation (Table 6) which showed low correlation for group IV. Therefore, MEA-neurochip results need to be discussed carefully for all drugs that are that are actively exported from the brain by transporters. Similarly also ondansetron is *in vivo* actively exported

Table 8
Comparison of effective concentrations used in the BBB and cytotoxicity experiments with cytotoxic concentrations determined by LDH release assay and effective concentrations in electrophysiology experiments.

Drug	Concentration for Blood brain barrier (μM)[a]	Predicted unbound brain concentration Cu,br (nM)[b]	Concentration 2D model for cytotoxicity[c]		Cytotoxicity 2D model LDH (%) after 1d [d] ±SD		Lowest concentration significantly changing electro-phys. parameters ($p \leqslant 0.005$)[e]	
			Low	High	Low	High	Spike rate	Burst duration
Amiodarone	5	n.d.	3.5 nM	1.25 μM	n.d	19 ± 12.5	1 pM	10 nM
Chlorpromazine	2	1.7–8.3	10 nM	2.5 μM	n.d	15 ± 4.5	100 nM	1 nM
Buflomedil	2	68–170	10 nM	6.25 μM	n.d	6 ± 1.2	1 nM	10 nM
Diazepam	5	4.6–46.3	100 pM	10 nM	11 ± 2.1	22 ± 2.9	1 pM	1 pM
Carbamazepine	40	1178–7069	2.5 μM	20 μM	6 ± 3.5	13 ± 2.8	50 μM	10 nM
Propofol	25	High	1 nM	6.4 μM	8 ± 1.0	12 ± 0.9	1 nM	1 pM
Cyclosporine A	1	3.1–12.6	250 nM	2 μM	12 ± 2.3	18 ± 5.4	1 nM	–
Cisplatinum	15	High	1 nM	1 μM	8 ± 4.1	15 ± 6.1	100 nM	500 μM
Ciprofloxacin	10	475–760	12.5 μM	100 μM	n.d	11 ± 0.9	1 mM	–
Loperamide	0.01	0.08–0.27	100 pM	10 μM	6 ± 3.8	n.d	1 nM	10 μM
Nadolol	1	1.8–45	10 nM	10 μM	n.d	21 ± 1.7	100 nM	10 nM
Ondansetron	1	25–247	1 nM	30 μM	8 ± 1.9	16 ± 2.7	10 nM	100 nM

[a] Clinically relevant concentrations used in BBB experiments, taken from Table 3.
[b] Predicted unbound brain concentrations, taken from Table 3; n.d. not detectable; "high" means that the BBB was damaged upon exposure to the concentration in the preceding column and the permeability high.
[c] Concentrations used for the cytotoxicity estimation for the 2D model, bold: these concentrations were also used for proteomics and metabolomics studies.
[d] Relative cytotoxicity values (estimated% cell loss) from released LDH measurements for 1 day exposure; for reasons discussed in Section 2.2. The cytotoxicity for long term exposure is probably higher so that we consider these only as estimates ($n = 3$); n.d. not detectable, i.e. 4% or less.
[e] Concentration levels at which significant changes in the electrical patterns were found upon acute exposure.

from the brain by pg-transporters (Schinkel et al., 1996). Therefore the effects including cytotoxicity (Table 8) which are observed in the 2D model culture are not in contradiction as in these studies the drugs have constantly free access to the networks.

The obtained free brain plasma ratios using the *in vitro* BBB model were used together with the unbound plasma concentration in human to predict the attainable unbound brain concentrations (Table 3). This illustrates that the applied *in vitro* approach has the potential to predict the level of unbound drug disposition in the brain in a single experiment and can be used to identify the compounds in the early drug discovery process that are most likely to elicit a neurotoxic effect.

However, the use of an *in vitro* model of human origin would be beneficial. The recent demonstration that human stem cells derived from umbilical cord blood can be differentiated into ECs displaying the BBB phenotype in coculture with brain pericytes (Cecchelli et al., 2014) opens up new opportunities toward the development of a brain neurovascular unit model with endothelial cells, pericytes, glial cells and neurons.

The drug-induced toxicity was further evaluated by applying integrated OMICs analysis (transcriptomics, proteomics and metabolomics) in combination with electrical activity measurements since those tools allow to study molecular mechanisms of neurotoxicity pathways. The major aim was to investigate the benefit of integrating OMICs data combined with functional neuronal specific endpoint (electrical activity) for application in drug safety, using an *in vitro* complementary neuronal test systems treated with the selected drugs in a repeated-exposure scheme.

4.2. Metabolomics

Gene expression and proteomics address the phenotypic adaptation of a cell but metabolite profiling can give an instantaneous snapshot of alterations in cell physiology. Based on the metabolomics data obtained from the 2D and 3D models exposed to the four drugs such as cyclosporine A, amiodarone, diazepam and chlorpromazine it can be concluded that the investigated drugs mostly affected the key neurotransmitters such as glutamate and 4-aminobutyrate and other amino acids, metabolically linked to neurotransmitters (glutamine, choline, aspartate, phenylalanine) or energy metabolism (malonate, succinate) however in different patterns with respect to time points and concentration. Diazepam as an example of non-toxic drugs induced less significant changes. Changes in metabolites associated with glutamate and succinic acid (TCA) metabolism have previously been associated with exposure of human embryonic stem cells (hESCs) to developmental toxicants (West et al., 2010). Aspartate (Choi et al., 1989) and glutamate (Hassel and Dingledine, 2006) are the main excitatory neurotransmitters that have been implicated in a number of pathologies of the nervous system (Meldrum, 2000; Platt, 2007) causing neuronal cell death through excitotoxicity (Bal-Price and Brown, 2001).

Minor alterations were seen in redox or other signaling pathways. Interestingly, in 2D cultures glutathione levels were down-regulated by all for drugs already at low concentrations, suggesting that oxidative stress could serve as early marker of neurotoxicity. However, further studies are needed to define a threshold that will allow discriminating between defense mechanisms and induced neurotoxicity.

In the case of the 3D model the levels of glutathione were down-regulated only by diazepam at both studied concentrations suggesting that the 3D model could express higher levels of defense mechanisms against oxidative stress. Several putatively annotated small molecules in the glutathione metabolism pathway showed also significant fold changes after exposure of hESCs to chemicals (Kleinstreuer et al., 2011). Glutathione is an important antioxidant, preventing damage to critical cellular components caused by oxidative stress (Balasz et al., 2014; Pompella et al., 2003). In its reduced state, it has the ability to protonate free radicals and thus acts as the major antioxidant defense mechanism against reactive oxygen species. There are studies showing that glutathione depletion and oxidative stress are strongly correlated with embryopathy in rats (Hansen et al., 2001) and humans (Zhao et al., 2006). A strong association between the glutathione pathway, oxidative stress and developmental defects was predicted by the environmental chemicals test set and supported by ToxCast data (Kleinstreuer et al., 2011).

In our studies a difference in response between 2D and 3D neuronal/glial models observed in metabolomics and proteomics, could be possibly due to the differences in neuronal and glial cell

composition, the state of cell differentiation and maturation or due to the different drug concentrations used because of the somewhat different sensitivities found for the three models here.

Interestingly, there are some metabolites that were down regulated in both neuronal models at the high concentration and the same time of exposure (Table 7, bold) and a few down-regulated in the same direction in both models at the same time point, but different concentrations of treatment (Table 7; not bold). These metabolites were regulated concomitantly in both models and could serve as potential candidates of a set of *in vitro* neurotoxicity biomarkers. The same metabolites were already suggested by van Vliet et al. (2008) as biomarkers of *in vitro* neurotoxicity induced by the exposure of rat brain aggregates to methyl mercury.

However, before a solid conclusion can be drawn more compounds (drugs and chemicals) have to be tested using the *in vitro* approach and the obtained results have to be compared with *in vivo* studies, followed by the mechanistic proof of relevance of the determined biomarkers to the *in vivo* human situation.

Generally, changes of these metabolites might be treated as an alert when exerted by potential neurotoxic drugs. However, in CNS-focused drug development, effects on the amino acid transmitters or their precursors may well be intended so careful consideration of wanted and unwanted metabolite changes is necessary by mechanism-based understanding of the metabolome. The evaluation of a higher number of known drugs is required to better determine the combination of metabolites that could be recognized as potential biomarkers of drug-induced neurotoxicity.

4.3. Proteomics

Since metabolites and protein expression changes could yield complementary information regarding drug-induced neurotoxic effects, they were both evaluated in parallel studies. However, few proteins showed the same alterations by exposure to the same drug in the 2D and the 3D neuronal models. This can be seen in a correlation analysis (Fig. SUPP 1 in the Supplementary Material), where proteins (less than 5%) equally up- or down-regulated would be located at or near the bisecting line. This indicates that each drug affects each cell model (2D and 3D) by various molecular mechanisms due to the differences between these two test systems as discussed above.

Interestingly, the proteomics data revealed that the drugs influenced protein expression relevant to both general and neuron-specific cell function. Based on an Ingenuity Pathway Analysis (IPA) study for the 2D *in vitro* model the profile of changed proteins hints toward different deregulated pathways and metabolic networks. In the case of chlorpromazine a possible upstream involvement of ubiquitin protein ligase E3A (UBE3A), glutamate receptor metabotropic 3 (GRM3) pathways/regulatory networks was identified. GRM3 encodes the metabotropic glutamate group II receptors (mGluR3) located pre- and post-synaptically and being mainly involved in presynaptic inhibition. L-Glutamate is the major excitatory neurotransmitter in the central nervous system and activates both ionotropic and metabotropic glutamate receptors (Petralia et al., 1996).

An IPA of the protein pattern changes induced by amiodarone indicated that the upstream function of MAPT, amyloid beta A4 protein (APP) and dysbindin (Dtnbp1) pathways could be affected (see Supplemental Material, Table SUPP 3). MAPT encoding the microtubule-associated protein tau (MAPT), a protein critical for axonal transport, was also deregulated by the exposure to cyclosporine A and diazepam. APP (amyloid beta (A4) precursor) encodes the protein that is cleaved by secretases to form a number of peptides (Tyan et al., 2012). Some of them promote transcriptional activation, while others form the amyloid plaques found in the brains of patients with Alzheimer's disease.

In the 3D model exposure to amiodarone caused upregulation of the neuronal specific protein, synaptogamin-10, the presynaptic protein involved in vesicle exocytosis, a process critical for the synaptic neurotransmission. Cyclosporine A decreased levels of MAP-6 which could affect the repression of neuron-specific genes in non-neuronal cells (Hakimi et al., 2002). Cyclosporine A also affected TP53-dependent transcriptional repression which leads to apoptosis (Fridman and Lowe, 2003) and affects cell-cycle regulation (Vogelstein et al., 2000).

A potential biomarker of neurotoxicity identified in the chlorpromazine study in 2D neuronal network cultures, could be up-regulation of excitatory amino acid transporter 1 (Eaat1, GLAST-1) involved in reuptake of the excitatory neurotransmitter glutamate. Eaat1 is highly expressed on astrocytes (but also neurons) in different brain structures and it is responsible for clearing excess glutamate from the extracellular space to avoid over-excitation of glutamate NMDA receptors which could lead to excitotoxicity and can eventually lead to cell death (Frega et al., 2012; Kirschner et al., 1994). Down-regulation of synphilin-1A and dynein was observed after exposure of brain aggregates to chlorpromazine. Dynein plays a critical role in axonal retrograde transport (Waterman-Storer et al., 1997) and synphilin-1 may contribute to neuronal degeneration in α-synucleopathies such as Parkinson's disease (Eyal et al., 2006).

Interestingly, many of these affected proteins are specific for neurons linked to neurotransmitter synthesis, synaptic vesicle transport, vesicle docking, vesicle exocytosis, postsynaptic receptors and glial cells such as transmitter reuptake from the synaptic cleft. Together with the metabolomics results this corroborates the view that neuron-specific transcription factors, amino acids and neurotransmitters and their fate in the neuron are main changes detectable by metabolomics and proteomics. Another consistent result was the fact that with all drugs the metabolic pathways and the upstream regulators found by IPA were identical for all low concentrations and the shorter exposure times of the low concentration of a given drug while only the high concentration for 14 days caused some changes in the pathways reported by the software (Table SUPP 3 in the Supplementary Material). This could indicate that at low concentrations cells cope with the treatments so that the effects may be rather homeostatic than toxic. Furthermore, acute neurotoxicity involves in many cases regulation at the receptor level which does not require changes in gene expression. This implies that proteomics studies are more suitable for the chronic repeated dose experiments while electrophysiology experiments are appropriate to search for short term neurotoxic effects.

Although the proteomics analyses were based on relatively few significant protein changes it can be seen that this approach together with IPA analyses gives first indications on possible molecular mechanisms of neurotoxicity. It is especially striking, how different the protein changes and the mechanisms proposed by IPA are among the different drugs. This indicates how finely regulated and how numerous the different neuronal and glial cell types in the nervous system are, which all differ in their metabolism, neurotransmitters and their receptor and signaling cascade patterns. Therefore, a multitude of potential drug targets is to be expected leading to drug-specific protein pattern changes. Clearly, more data need to be collected for the omics approaches to identify readily usable biomarkers based on adverse outcome pathways, many more chemicals will need to be tested across a wider concentration range, and both *in vivo* and *in vitro* experiments will be required to finally establish the pathways and biomarkers that are reliable and predictive for neurotoxicity.

4.4. Analysis of electrical activity patterns

The changes of neurotransmitters and their synaptic transmission-related protein machinery observed in proteomics and metabolomics analyses should also be reflected by changes in the electrical activity of neuronal ensembles. Therefore, the effects of the 12 selected drugs on the action potential patterns in the neuronal network cultures (2D model) were analyzed for its predictivity for neurotoxicity.

Already with only 12 drugs divided into four groups of neuroactive and neurotoxic compounds for which a dataset of 200 acute concentration–response curves (electrical activity fingerprint) was established the drugs were almost all classified correctly which means that specific fingerprints of activity patterns for each class can be identified. The incomplete separation of drugs of class II and IV may be explained by the heterogeneity of the compounds grouped together in a preliminary way for training the data classification algorithm in this study. The obtained data suggest that functional acute neurotoxicity evaluation based on activity "fingerprints" derived at low or non-cytotoxic concentrations after acute exposure (Fig. 6) will be a reliable tool for *in vitro* drug-induced neurotoxicity testing. Although preliminary experiments have shown that the MEA technology is suited for repeated exposure and for developmental neurotoxicity evaluation (Hogberg et al., 2011; Robinette et al., 2011), its major application may well be in acute toxicity studies. It has to be further developed with a larger set of reference compounds to show how robust acute neurotoxicity analyses are for this endpoint.

Compared to conventional assays the electrophysiological evaluation could provide an early predictive, functional and sensitive endpoint especially for *in vitro* neurotoxicity testing during early drug development. In multivariate *pharmacological* testing this classification approach has already proven to be a valuable tool permitting the identification of drugs with different sets of of activity changes which can be directly assigned to pharmacological mechanisms and drug targets (anticonvulsants: Gramowski et al., 2004; opioids: Parenti et al., 2013; Vandormael et al., 2011; antidepressants: Gramowski et al., 2006). It is demonstrated here that a set of such measurements has an information content high enough to form the basis for classifying and discriminating the different drugs according to their *neurotoxic* potential. It can be considered as a *proof of concept* that the differences recognized are sufficient for the classification, which will become more distinctive when data on more drugs and toxins are becoming available.

MEA analysis is a non-invasive, label-free, high content technology which has been utilized for neurotoxicity monitoring of both acute and chronic effects of drugs and toxins (Gramowski et al., 2011; Johnstone et al., 2010; Shafer et al., 2008; Weiss, 2011) including developmental neurotoxicity (Hogberg et al., 2011). Its potential was further demonstrated in a study of 30 selected compounds using multi-well MEAs that induced neurotoxic effects by a broad variety of different mechanisms (McConnell et al., 2012). An intra-laboratory reproducibility and inter-laboratory variability study of MEA measurements performed in six different laboratories (Novellino et al., 2011) showed that it is a robust functional endpoint suitable for *in vitro* studies of neurotoxicity.

Simplified versions of MEA technology which use only one parameter (spike rate) or one or few concentrations (e.g. 50 μM) have been tested recently to obtain yes-or-no answers on neuro/cytotoxicity of chemicals as required for REACH testing (Registration, Evaluation, Authorisation and Restriction of Chemicals) (Defranchi et al., 2011; Lefew et al., 2013; McConnell et al., 2012; Valdivia et al., 2014). Such univariate tests can use Bayesian modeling to improve the results but no insight into mechanisms or subclassification of the chemicals can be obtained. Much more information is gained from multivariate analyses by deriving many parameters which require the application of more advanced data analysis than Bayesian modeling (6 parameters: Frega et al., 2012; 14 parameters and classification by support vector machines and Principal Component Analysis: Mack et al., 2014; 200 parameters and classification by support vector machines, neural network and machine learning algorithms: this study and Parenti et al., 2013).

The refined data analysis and classification methods which can be based on substance fingerprints that are defined by up to 200 concentration response curves over the full concentration range as it was used here not only classified the 12 tested drugs correctly into 4 groups with respect to their toxic potential, but would give valuable information on drug mechanisms (toxicological or pharmacological) if their fingerprints are further processed. This can be reached by classifying the complete electrical signature of a drug against a library which contains the signatures of compounds with known toxic or pharmacological effects (Johnstone et al., 2010). Therefore, using the MEA technology to its full extent is especially recommended for neurotoxicity analyses during early drug development as it provides not only a "toxicological fingerprint" but from the same data set also a "pharmacological fingerprint" can be obtained, giving added value to this approach.

In Table 8 the predicted unbound brain concentration as obtained from the BBB part of this work (Table 3), the cytotoxicity estimation (see also Fig. 2A and Fig. SUPP 3) and the concentration level at which significant changes in the electrical patterns were found (MEA experiments, see Fig. 6 and Fig. SUPP 2) are presented for the cortical neuronal/glial network model (2D model) for comparison.

For planning *in vitro* neurotoxicity evaluations it is not relevant to use concentrations that are relevant to clinically determined human blood concentrations (Table 8, column 2). Due to the absence of the BBB, the predicted unbound brain concentrations (Table 8, column 3) have to be used instead when substances are tested *in vitro* for comparison relevant to the *in vivo* situation. Comparing the concentrations used in our study for estimating cytotoxicity with the predicted brain concentrations it is seen that for some drugs at 1 day of exposure at the low concentrations no cytotoxic effects are to be expected (chlorpromazine, buflomedil, ciprofloxacin and nadolol) while others (diazepam, carbamazepine, loperamide, ondansetron) may cause some cytotoxicity. The concentrations used for the OMICs studies (Table 1) were higher than the predicted unbound brain concentrations as lower concentrations induced only few significant changes.

Concentration levels at which significant changes in the electrical patterns were found upon acute exposure in the 2D model for the two example parameters "spike rate" and "burst duration" (Table 6) are indeed in the same range as expected brain concentrations (Table 8). The threshold of significant changes appears for several of the tested drugs at or below detectable cytotoxicity (chlorpromazine, buflomedil). It should also be noted that some of the other parameters out of the 200 used for classification calculations may be even more sensitive. It is, therefore, considered adequate to use these endpoints to very sensitively predict functional changes in the CNS even in cases where the BBB is intact (chlorpromazine, buflomedil, diazepam, carbamazepine, nadolol and ondansetron), because the predicted unbound brain concentrations are in the same range as the low concentration where significant changes were seen in the 2D electrophysiological experiments (Table 8). However, studies of the BBB permeability would need to be performed in conjunction in order to obtain the unbound brain concentrations.

4.5. Integrated testing strategy (ITS)

The main aim of the PREDICT-IV project was to apply advanced tools as OMICs technologies and high-content analysis to improve the early identification of toxic effects, including neurotoxicity. Based on the obtained results an *in vitro* ITS for drug-induced neurotoxicity evaluation has been proposed (Table 9) based on complementary *in vitro* mixed neuronal/glial models (with the presence of glial cells) and a battery of endpoints that will allow neurotoxicity evaluation in a robust, sensitive and quantitative manner. In this project two neuronalglial primary cultures (2D and 3D) were evaluated to determine how these two test systems could be used in a complementary manner taking into consideration the advantages of each model. Additionally, the *in vitro* BBB model was applied to determine when and why a BBB model should be included in the proposed ITS (Table 9).

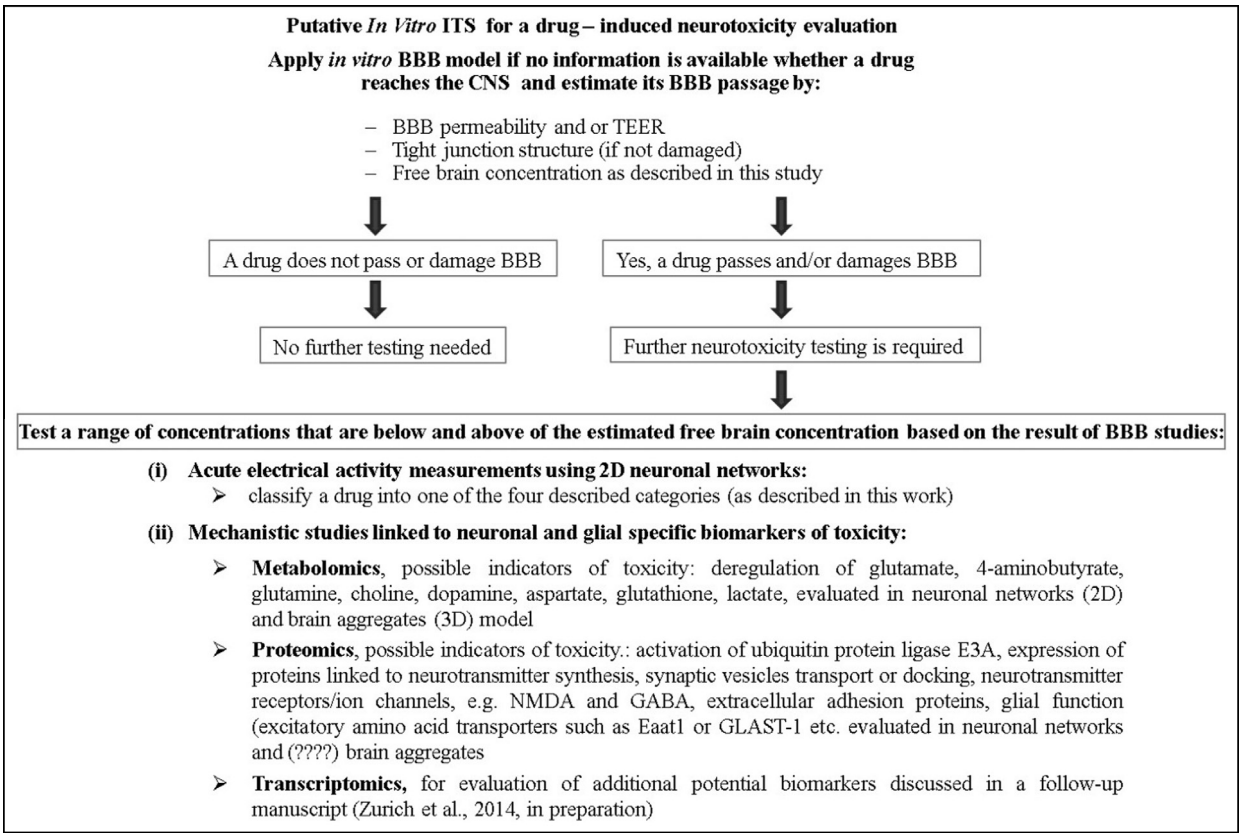
In drug-induced neurotoxicity evaluation, the first question to be answered is whether a compound is reaching the brain, and if so at what concentration. *In vitro* BBB studies allowed the estimation of the actual drug concentration that is reaching the target, brain cells. The proposed approach is based on the calculation of the unbound brain/plasma ratio generated *in vitro* and estimated plasma exposure permits to make an early prediction of the risk of a toxicological effect in the human CNS (Table 9). The *in vitro* free brain plasma ratio which is used to predict pharmacological effects *in vivo* was successfully applied here for the first time in a repeated exposure regime (14 days) and it was proved that it is possible to use this method to predict a drug brain free concentrations. This information is a prerequisite to predict the toxic potential of drugs studied *in vitro*. The passage of a drug through the BBB or a direct damage of the BBB by a drug can be evaluated by measurements of BBB permeability (as described in this work) or by TEER measurements (e.g. Boveri et al., 2006). If a drug does neither pass the BBB, nor damages it, this drug can be recognized as not neurotoxic and further testing is not needed (Table 9). However, if a drug passes the BBB nor damages it this compound then further toxicity testing is required (Table 9). Based on the *in vitro* BBB studies the relevant compound concentrations should be selected taking into consideration *in vitro* drug's pharmacokinetic behavior to determine a free drug concentration in the culture medium to which the cells are exposed (after deduction of a compound binding to plastic, serum proteins etc.).

A range of concentrations that are below and above of the estimated free brain concentrations should be first evaluated by electrical activity measurements after acute exposure followed up by OMICs analysis or other mechanistic studies (Table 9) applied to long term treatments that will allow more in depth evaluation of the triggered pathways of toxicity.

The applied metabolomics and proteomics studies to 2D and 3D models permit to suggest potential neuronal-specific biomarkers, identified among deregulated metabolites and proteins specific for neuronal and glial pathways of toxicity (as discussed above). Further biomarkers were identified based on transcriptomics studies (data not shown) that will be discussed in a separate paper (Zurich and Bal-Price, 2015). Taking all results together (OMICs analysis and electrical activity measurements) should allow functional evaluation after acute exposure and the determination of pathways of toxicity after long term treatment, leading to identification of biomarkers specific for drug/chemical induced neurotoxicity.

It should be noted that for a single measurement OMICs assays have become relatively cheap and will become even cheaper by

Table 9
Proposed *in vitro* ITS for drug – induced neurotoxicity evaluation.



automated assays. The same trend is seen in MEA assays, which are available in 48 and 96 well format, so the cost is already in the same order of magnitude.

However, to validate the putative biomarkers of neurotoxicity identified in this study, *in vivo* experiments have to be performed with the same drugs and extrapolation to human exposure have to be performed. Since *in vivo* data (especially human data) do not exist, the suggested biomarkers are only indicative and need further confirmation. Therefore, *in vivo* and *in vitro* studies with a larger number of chemicals (negative and positive controls) have to be performed to establish the toxicity pathways and identify reliable biomarkers of predictive neurotoxicity.

In conclusion, metabolomics and proteomics could deliver highly predictive data, if neuro-therapeutic relevant changes could be separated from neurotoxic ones with well-defined compounds and concentrations as references for calibration. Therefore, as a follow-up of this project, the criteria for *in vitro* neurotoxicity testing should be identified which allow discrimination between physiology, pharmacology and neurotoxicology of a studied drug or chemical. Such thresholds for positive hits should also be defined for neuronal electrical activity changes to facilitate further interpretation of the obtained data in a quantitative manner.

The results obtained by functional, initial screening using the MEA neurochips appear to be useful as an early standard screen for identification of acute neurotoxicity and prioritization of chemicals/drugs with neurotoxic potential. However, based on the PREDICT-IV project results it is not clear whether this endpoint is suitable for studying long-term exposure and obviously it does not give direct information on the toxicity pathways that are behind the observed neurotoxicity. This may, in principle be achievable, if pathway-specific electrical patterns changes are established in the future. Therefore, currently acute neurotoxicity evaluation based on the initial electrical activity studies should be followed by mechanistic studies (e.g. OMICs analyses) or other mechanistic studies performed after long term exposure to determine adverse outcome pathways (AOP) that could be further used for regulatory purposes (Bal-Price et al., 2015a,b).

In the context of drug-induced neurotoxicity testing it is suggested that future MEA research activities should be intensified toward data analysis and pattern recognition linked to specific neurological pathologies or psychopathologies that could be induced as side effects by certain drugs, such as depression, dementia, insomnia, anxiety or degenerative disorders.

Since neurotoxicity may occur by a number of different mechanisms, it is necessary to build *in vitro* ITS based on the complementary neuronal models and battery of endpoints covering the most fundamental mechanisms of neurotoxicity (Bal-Price et al., 2010). In this project the applied CNS models are complementary as the 2D model consisting of cortical neuronal networks on MEA neurochips are best suited for the electrophysiological evaluation after acute exposure, the 3D re-aggregating culture model is better suitable for biochemical, enzymological and OMICs studies due to its more physiological cellular arrangement and larger amount of available material (Zurich et al., 2013), suitable for both acute and long term treatment. As shown here, the two models differ considerably as they come from two different species (rat and mouse), with respect to percentage of the different cell types, cellular architecture, cell–cell and cell–extracellular matrix connections, structural size and density (possibly influencing drug accessibility). The 3D cultures stand out due to the presence of compact myelin and microglial cells supporting neuroinflammatory and neuroprotective processes (Monnet-Tschudi et al., 2007). The models are complementary because they are amenable to yield insight into possible disturbances covering together a variety of different neuron- and glia-specific mechanisms and functions of the CNS.

This study demonstrated that the *in vitro* neuronal cell culture systems coupled with functional electrical activity measurements and high content OMICs approaches can give detailed insights into both the pharmacological and toxicological effects of drugs after both acute and long term exposure. Both proteomics and metabolomics indicated which general and neuronal/glial specific pathways are possibly affected by a drug. In addition, *in vitro* BBB model provided information whether toxicity was induced at the BBB level and facilitated a prediction of brain concentrations of unbound drug. Based on these results, it is suggested that the *in vitro* BBB model should be included in such ITS especially when a new compound is tested where data on the BBB transport and brain concentrations have to be defined.

As has recently been widely discussed (NRC 2007) there is a need for a profound shift in toxicity testing (including neurotoxicity) for drugs and chemicals as using animal models followed up by the extrapolation across species is not always leading to reliable results which are relevant to human exposure. Recent approaches are focused on the study of pathways of toxicity using human cell models derived from human pluripotent stem cells (hPSCs) (embryonic but preferably induced). There is significant progress in differentiating hPSCs into mixed neuronal/glial cultures for subsequent application to *in vitro* neurotoxicity testing (Pistollato et al., 2012). Hopefully, in the near future, the proposed ITS for drug-induced neurotoxicity evaluation can be based on human stem cell-derived neuronal models.

In conclusion, an integrated OMICs approach combined with a functional electrical activity evaluation and an *in vitro* BBB model as well as stable *in vitro* neuronal/glial cell culture models (in the future preferably human-derived neuronal test systems) has the potential to considerably advance our understanding of drug/chemical-induced cellular perturbations. With this knowledge it should be possible to establish a reliable, integrated testing strategy for predicting human *in vitro* neurotoxicity.

Conflict of Interest

The authors declare that there are no conflicts of interest.

Transparency Document

The Transparency document associated with this article can be found in the online version.

Acknowledgements

This work was performed within the Large-Scale Integrating Project PREDICT IV, "Profiling the toxicity of new drugs: A non animal-based approach integrating toxico-dynamics and biokinetics" funded by the EU 7th Framework Programme (Contract No. 202222). http://www.predict-iv.toxi.uni-wuerzburg.de. We thank Hannelore Popa-Henning for the administrative work and organization. The excellent technical support of Kristine Gürtler, Rachid Aïjjou, Johan Hachani, Denise Tavel and Brigitte Delacuisine is gratefully acknowledged.

Appendix A. Supplementary material

Supplementary data associated with this article can be found, in the online version, at http://dx.doi.org/10.1016/j.tiv.2015.05.016.

References

Agid, Y., Buzsaki, G., Diamond, D.M., Frackowiak, R., Giedd, J., et al., 2007. How can drug discovery for psychiatric disorders be improved? Nat. Rev. Drug Discov. 6, 189–201.

Bal-Price, A., Brown, G.C., 2001. Inflammatory neurodegeneration mediated by nitric oxide from activated glia-inhibiting neuronal respiration, causing glutamate release and excitotoxicity. J. Neurosci. 21, 6480–6491.

Bal-Price, A.K., Hogberg, H.T., Buzanska, L., Coecke, S., 2010. Relevance of in vitro neurotoxicity testing for regulatory requirements: challenges to be considered. Neurotoxicol. Teratol. 32, 36–41.

Bal-Price, A.K., Coecke, S., Costa, L., Crofton, K.M., Fritsche, E., et al., 2012. Advancing the science of developmental neurotoxicity (DNT): testing for better safety evaluation. ALTEX 29, 202–215.

Bal-Price, A., Crofton, K.M., Sachana, M., Shafer, T.J., Behl, M., et al., 2015a. Putative adverse outcome pathways (AOP) relevant to neurotoxicity. Crit. Rev. Toxicol. 45 (1), 83–91.

Bal-Price, A., Crofton, Kevin, Leist, Marcel, Allen, Sandra, Arand, Michael, et al., 2015b. International STakeholder NETwork (ISTNET): creating a Developmental Neurotoxicity (DNT) testing roadmap for regulatory purposes. Arch. Toxicol. 89, 269–287.

Balasz, M., Szkilnik, R., Brus, R., Malinowska-Borowska, J., Kasperczyk, S., et al. 2014. Perinatal manganese exposure and hydroxyl radical formation in rat brain. Neurotoxicity research.

Becker, S., Liu, X., 2006. Evaluation of the utility of brain slice methods to study brain penetration. Drug Metab. Dispos.: Biol. Fate Chem. 34, 855–861.

Bellwon, P., Culot, M., Wilmes, A., Schmidt, T., Zurich, M., et al., 2015. Cyclosporine A kinetics in brain cell cultures and its potential of crossing the blood–brain barrier. Toxicol. In Vitro 30, 166–175.

Boveri, M., Kinsner, A., Berezowski, V., Lenfant, A.M., Draing, C., et al., 2006. Highly purified lipoteichoic acid from gram-positive bacteria induces in vitro blood-brain barrier disruption through glia activation: role of pro-inflammatory cytokines and nitric oxide. Neuroscience 137, 1193–1209.

Booher, J., Sensenbrenner, M., 1972. Growth and cultivation of dissociated neurons and glial cells from embryonic chick, rat and human brain in flask cultures. Neurobiology 2, 97–105.

Breitwieser, F.P., Muller, A., Dayon, L., Kocher, T., Hainard, A., et al., 2011. General statistical modeling of data from protein relative expression isobaric tags. J. Proteome Res. 10, 2758–2766.

Cao, P., Maximov, A., Sudhof, T.C., 2011. Activity-dependent IGF-1 exocytosis is controlled by the Ca(2+)-sensor synaptotagmin-10. Cell 145, 300–311.

Cecchelli, R., Dehouck, B., Descamps, L., Fenart, L., Buee-Scherrer, V.V., et al., 1999. In vitro model for evaluating drug transport across the blood–brain barrier. Adv. Drug Deliv. Rev. 36, 165–178.

Cecchelli, R., Aday, S., Sevin, E., Almeida, C., Culot, M., et al., 2014. A stable and reproducible human blood–brain barrier model derived from hematopoietic stem cells. PloS one 9, e99733.

Chapman, E.R., 2002. Synaptotagmin: a Ca(2+) sensor that triggers exocytosis? Nat. Rev. Mol. Cell Biol. 3, 498–508.

Choi, D.W., Viseskul, V., Amirthanayagam, M., Monyer, H., 1989. Aspartate neurotoxicity on cultured cortical neurons. J. Neurosci. Res. 23, 116–121.

Coecke, S., Ahr, H., Blaauboer, B.J., Bremer, S., Casati, S., et al., 2006a. Metabolism: a bottleneck in in vitro toxicological test development. The report and recommendations of ECVAM workshop 54. Altern. Lab. Animals: ATLA 34, 49–84.

Coecke, S., Eskes, C., Gartlon, J., Kinsner, A., Price, A., et al., 2006b. The value of alternative testing for neurotoxicity in the context of regulatory needs. Environ. Toxicol. Pharmacol. 21, 153–167.

Craig, R., Beavis, R.C., 2004. TANDEM: matching proteins with tandem mass spectra. Bioinformatics 20, 1466–1467.

Cremona, O., Di Paolo, G., Wenk, M.R., Luthi, A., Kim, W.T., et al., 1999. Essential role of phosphoinositide metabolism in synaptic vesicle recycling. Cell 99, 179–188.

Crofton, K.M., Mundy, W.R., Lein, P.J., Bal-Price, A., Coecke, S., et al., 2011. Developmental neurotoxicity testing: recommendations for developing alternative methods for the screening and prioritization of chemicals. ALTEX 28, 9–15.

Csermely, P., Korcsmaros, T., Kiss, H.J., London, G., Nussinov, R., 2013. Structure and dynamics of molecular networks: a novel paradigm of drug discovery: a comprehensive review. Pharmacol. Therap. 138, 333–408.

Culot, M., Lundquist, S., Vanuxeem, D., Nion, S., Landry, C., et al., 2008. An in vitro blood–brain barrier model for high throughput (HTS) toxicological screening. Toxicol. In Vitro: Int. J. Publ. Assoc. BIBRA 22, 799–811.

Culot, M., Fabulas-da Costa, A., Sevin, E., Szorath, E., Martinsson, S., et al., 2013. A simple method for assessing free brain/free plasma ratios using an in vitro model of the blood brain barrier. PloS one 8, e80634.

Cummings, J.L., Morstorf, T., Zhong, K., 2014. Alzheimer's disease drug-development pipeline: few candidates, frequent failures. Alzheimer's Res. Therapy 6, 37.

Defranchi, E., Novellino, A., Whelan, M., Vogel, S., Ramirez, T., et al., 2011. Feasibility assessment of micro-electrode chip assay as a method of detecting neurotoxicity in vitro. Front. Neuroeng. 4, 6.

Dehouck, M.P., Meresse, S., Delorme, P., Fruchart, J.C., Cecchelli, R., 1990. An easier, reproducible, and mass-production method to study the blood–brain barrier in vitro. J. Neurochem. 54, 1798–1801.

Eyal, A., Szargel, R., Avraham, E., Liani, E., Haskin, J., et al., 2006. Synphilin-1A: an aggregation-prone isoform of synphilin-1 that causes neuronal death and is present in aggregates from alpha-synucleinopathy patients. Proc. Natl. Acad. Sci. USA 103, 5917–5922.

Fabulas-da Costa, A., Aijjou, R., Hachani, J., Landry, C., Cecchelli, R., Culot, M., 2013. In vitro blood–brain barrier model adapted to repeated-dose toxicological screening. Toxicol. In Vitro: Int. J. Publ. Assoc. BIBRA 27, 1944–1953.

Frega, M., Pasquale, V., Tedesco, M., Marcoli, M., Contestabile, A., et al., 2012. Cortical cultures coupled to micro-electrode arrays: a novel approach to perform in vitro excitotoxicity testing. Neurotoxicol. Teratol. 34, 116–127.

Friden, M., Gupta, A., Antonsson, M., Bredberg, U., Hammarlund-Udenaes, M., 2007. In vitro methods for estimating unbound drug concentrations in the brain interstitial and intracellular fluids. Drug Metab. Dispos.: Biol. Fate Chem. 35, 1711–1719.

Fridman, J.S., Lowe, S.W., 2003. Control of apoptosis by p53. Oncogene 22, 9030–9040.

Fung, M., Thornton, A., Mybeck, K., Wu, J.H.-H., Hornbuckle, K., Muniz, E., 2001. Evaluation of the characteristics of safety withdrawal of prescription drugs from worldwide pharmaceutical markets-1960 to 1999. Drug Inform. J. 35, 293–317.

Geer, L.Y., Markey, S.P., Kowalak, J.A., Wagner, L., Xu, M., et al., 2004. Open mass spectrometry search algorithm. J. Proteome Res. 3, 958–964.

Gramowski, A., Jugelt, K., Weiss, D.G., Gross, G.W., 2004. Substance identification by quantitative characterization of oscillatory activity in murine spinal cord networks on microelectrode arrays. Eur. J. Neurosci. 19, 2815–2825.

Gramowski, A., Jugelt, K., Stuwe, S., Schulze, R., McGregor, G.P., et al., 2006. Functional screening of traditional antidepressants with primary cortical neuronal networks grown on multielectrode neurochips. Eur. J. Neurosci. 24, 455–465.

Gramowski, A., Flossdorf, J., Bhattacharya, K., Jonas, L., Lantow, M., et al., 2010. Nanoparticles induce changes of the electrical activity of neuronal networks on microelectrode array neurochips. Environ. Health Perspect. 118, 1363–1369.

Gramowski, A., Jugelt, K., Schroder, O.H., Weiss, D.G., Mitzner, S., 2011. Acute functional neurotoxicity of lanthanum(III) in primary cortical networks. Toxicol. Sci.: Off. J. Soc. Toxicol. 120, 173–183.

Gross, G., Gopal, K., 2006. Emerging histiotypic properties of cultured neuronal networks. In: Taketani, M., Baudry, M. (Eds.), Advances in Network Electrophysiology. Springer, US, pp. 193–214.

Gross, G.W., Rhoades, B.K., Reust, D.L., Schwalm, F.U., 1993. Stimulation of monolayer networks in culture through thin-film indium-tin oxide recording electrodes. J. Neurosci. Meth. 50, 131–143.

Gross, G.W., Harsch, A., Rhoades, B.K., Gopel, W., 1997. Odor, drug and toxin analysis with neuronal networks in vitro: extracellular array recording of network responses. Biosensors Bioelectron. 12, 373–393.

Hakimi, M.A., Bochar, D.A., Chenoweth, J., Lane, W.S., Mandel, G., Shiekhattar, R., 2002. A core-BRAF35 complex containing histone deacetylase mediates repression of neuronal-specific genes. Proc. Natl. Acad. Sci. USA 99, 7420–7425.

Hallier-Vanuxeem, D., Prieto, P., Culot, M., Diallo, H., Landry, C., et al., 2009. New strategy for alerting central nervous system toxicity: integration of blood–brain barrier toxicity and permeability in neurotoxicity assessment. Toxicol. In Vitro: Int. J. Publ. Assoc. BIBRA 23, 447–453.

Hansen, J.M., Carney, E.W., Harris, C., 2001. Altered differentiation in rat and rabbit limb bud micromass cultures by glutathione modulating agents. Free Radical Bio. Med. 31, 1582–1592.

Harry, G.J., Tiffany-Castiglioni, E., 2005. Evaluation of neurotoxic potential by use of in vitro systems. Expert Opin. Drug Metab. Toxicol. 1, 701–713.

Hassel, B., Dingledine, R., 2006. Glutamate. In: Brady, S., Siegel, G., Albers, R.W., Price, D. (Eds.), Basic Neurochemistry: Molecular, Cellular and Medical Aspects. Elsevier Academic Press, pp. 268–290.

Hodel, A., 1998. SNAP-25. Int. J. Biochem. Cell Biol. 30, 1069–1073.

Hogberg, H.T., Sobanski, T., Novellino, A., Whelan, M., Weiss, D.G., Bal-Price, A.K., 2011. Application of micro-electrode arrays (MEAs) as an emerging technology for developmental neurotoxicity: evaluation of domoic acid-induced effects in primary cultures of rat cortical neurons. Neurotoxicology 32, 158–168.

Honegger, P., Zurich, M.G., 2011. Preparation and use of serum-free aggregating brain cell cultures for routine neurotoxicity screening. In: Aschner, M., Suñol, C., Bal-Price, A. (Eds.), Cell Culture Techniques. Humana Press, New York, pp. 105–128.

Honegger, P., Lenoir, D., Favrod, P., 1979. Growth and differentiation of aggregating fetal brain cells in a serum-free defined medium. Nature 282, 305–308.

Huettner, J.E., Baughman, R.W., 1986. Primary culture of identified neurons from the visual cortex of postnatal rats. J. Neurosci.: Off. J. Soc. Neurosci. 6, 3044–3060.

Johnstone, A.F., Gross, G.W., Weiss, D.G., Schroeder, O.H., Gramowski, A., Shafer, T.J., 2010. Microelectrode arrays: a physiologically based neurotoxicity testing platform for the 21st century. Neurotoxicology 31, 331–350.

Judson, R., Kavlock, R., Martin, M., et al., 2013. Perspectives on validation of high-throughput assays supporting 21st century toxicity testing. ALTEX 30, 51–56.

Kalvass, J.C., Maurer, T.S., 2002. Influence of nonspecific brain and plasma binding on CNS exposure: implications for rational drug discovery. Biopharm. Drug Dispos. 23, 327–338.

Keefer, E.W., Gramowski, A., Gross, G.W., 2001. NMDA receptor-dependent periodic oscillations in cultured spinal cord networks. J. Neurophysiol. 86, 3030–3042.

Kirschner, M.A., Arriza, J.L., Copeland, N.G., Gilbert, D.J., Jenkins, N.A., et al., 1994. The mouse and human excitatory amino acid transporter gene (EAAT1) maps to mouse chromosome 15 and a region of syntenic homology on human chromosome 5. Genomics 22, 631–633.

Kleinjans, J., 2014. Toxicogenomics-based Cellular Models. Alternatives to Animal Testing for Safety Assessment. MA, USA.

Kleinstreuer, N.C., Smith, A.M., West, P.R., Conard, K.R., Fontaine, B.R., et al., 2011. Identifying developmental toxicity pathways for a subset of ToxCast chemicals using human embryonic stem cells and metabolomics. Toxicology and applied pharmacology 257, 111–121.
Koh, J.Y., Choi, D.W., 1987. Quantitative determination of glutamate mediated cortical neuronal injury in cell culture by lactate dehydrogenase efflux assay. J. Neurosci. Meth. 20, 83–90.
Kola, I., Landis, J., 2004. Can the pharmaceutical industry reduce attrition rates? Nat. Rev. Drug Discov. 3, 711–715.
Lafuente-Lafuente, C., Alvarez, J.-C., Leenhardt, A., Mouly, S., Extramiana, F., et al., 2009. Amiodarone concentrations in plasma and fat tissue during chronic treatment and related toxicity. British J. Clin. Pharmacol. 67, 511–519.
Landesmann, B., Mennecozzi, M., Berggren, E., Whelan, M., 2013. Adverse outcome pathway-based screening strategies for an animal-free safety assessment of chemicals. Altern. Lab. Animals: ATLA 41, 461–471.
Lefew, W.R., McConnell, E.R., Crooks, J.L., Shafer, T.J., 2013. Evaluation of microelectrode array data using Bayesian modeling as an approach to screening and prioritization for neurotoxicity testing. Neurotoxicology 36, 34–41.
Leist, M., Hasiwa, N., Rovida, C., et al., 2014. Consensus report on the future of animal-free systemic toxicity testing. ALTEX 31, 341–356.
Mack, C.M., Lin, B.J., Turner, J.D., Johnstone, A.F., Burgoon, L.D., Shafer, T.J., 2014. Burst and principal components analyses of MEA data for 16 chemicals describe at least three effects classes. Neurotoxicology 40, 75–85.
McConnell, E.R., McClain, M.A., Ross, J., Lefew, W.R., Shafer, T.J., 2012. Evaluation of multi-well microelectrode arrays for neurotoxicity screening using a chemical training set. Neurotoxicology 33, 1048–1057.
Meldrum, B.S., 2000. Glutamate as a neurotransmitter in the brain: review of physiology and pathology. J. Nutr. 130, 1007s–1015s.
Meresse, S., Dehouck, M.P., Delorme, P., Bensaid, M., Tauber, J.P., et al., 1989. Bovine brain endothelial cells express tight junctions and monoamine oxidase activity in long-term culture. J. Neurochem. 53, 1363–1371.
Monnet-Tschudi, F., Zurich, M.G., Asher, R., Honegger, P., 1993. Glial hyaluronate-binding protein expression in aggregating brain cell cultures. Develop. Neurosci. 15, 395–402.
Monnet-Tschudi, F., Zurich, M.G., Honegger, P., 2007. Neurotoxicant-induced inflammatory response in three-dimensional brain cell cultures. Hum. Exp. Toxicol. 26, 339–346.
Montesinos, R.N., Moulari, B., Gromand, J., Beduneau, A., Lamprecht, A., Pellequer, Y., 2014. Coadministration of P-glycoprotein modulators on loperamide pharmacokinetics and brain distribution. Drug Metab. Dispos.: Biol. Fate Chem. 42, 700–706.
Nahnsen, S., Bertsch, A., Rahnenfuhrer, J., Nordheim, A., Kohlbacher, O., 2011. Probabilistic consensus scoring improves tandem mass spectrometry peptide identification. J. Proteome Res. 10, 3332–3343.
Namikawa, K., Asakura, M., Minami, T., Okazaki, Y., Kadota, E., Hashimoto, S., 2000. Toxicity of cisplatin to the central nervous system of male rabbits. Biol. Trace Element Res. 74, 223–235.
Nemes, P., Rubakhin, S.S., Aerts, J.T., Sweedler, J.V., 2013. Qualitative and quantitative metabolomic investigation of single neurons by capillary electrophoresis electrospray ionization mass spectrometry. Nat. Protocols 8, 783–799.
Novellino, A., Scelfo, B., Palosaari, T., Price, A., Sobanski, T., et al., 2011. Development of micro-electrode array based tests for neurotoxicity: assessment of interlaboratory reproducibility with neuroactive chemicals. Front. Neuroeng. 4, 4.
Parenti, C., Turnaturi, R., Arico, G., Gramowski-Voss, A., Schroeder, O.H., et al., 2013. The multitarget opioid ligand LP1's effects in persistent pain and in primary cell neuronal cultures. Neuropharmacology 71, 70–82.
Perkins, D.N., Pappin, D.J., Creasy, D.M., Cottrell, J.S., 1999. Probability-based protein identification by searching sequence databases using mass spectrometry data. Electrophoresis 20, 3551–3567.
Petralia, R.S., Wang, Y.X., Niedzielski, A.S., Wenthold, R.J., 1996. The metabotropic glutamate receptors, mGluR2 and mGluR3, show unique postsynaptic, presynaptic and glial localizations. Neuroscience 71, 949–976.
Pistollato, F., Bremer-Hoffmann, S., Healy, L., Young, L., Stacey, G., 2012. Standardization of pluripotent stem cell cultures for toxicity testing. Expert Opin. Drug Metab. Toxicol. 8, 239–257.
Platt, S.R., 2007. The role of glutamate in central nervous system health and disease – a review. Veterinary J. 173, 278–286 (London, England: 1997).
Pompella, A., Visvikis, A., Paolicchi, A., De Tata, V., Casini, A.F., 2003. The changing faces of glutathione, a cellular protagonist. Biochem. Pharmacol. 66, 1499–1503.
Pomponio, G., Zurich, M., Schultz, L., Weiss, D.G., Romanelli, L., et al., 2015. Amiodarone biokinetics in brain cell cultures and the formation of its major oxidative metabolite after repeated exposure. Toxicol. In Vitro: Int. J. Publ. Assoc. BIBRA.
Ransom, B.R., Neale, E., Henkart, M., Bullock, P.N., Nelson, P.G., 1977. Mouse spinal cord in cell culture. I. Morphology and intrinsic neuronal electrophysiologic properties. J. Neurophysiol. 40, 1132–1150.
Regenthal, R., Krueger, M., Koeppel, C., Preiss, R., 1999. Drug levels: therapeutic and toxic serum/plasma concentrations of common drugs. J. Clin. Monit. Comput. 15, 529–544.
Riedmiller M, Braun H. 1993. Neural networks, IEEE International Conference on 1993. 1, 586–591.
Robinette, B.L., Harrill, J.A., Mundy, W.R., Shafer, T.J., 2011. In vitro assessment of developmental neurotoxicity: use of microelectrode arrays to measure functional changes in neuronal network ontogeny. Front. Neuroeng. 4, 1–10.
Rovida, C., Alépée, N., Api, A.M., Basketter, D.A., Bois, F.Y., et al., 2015. Integrated Testing Strategies (ITS) for safety assessment. ALTEX 32 (1), 25–40.
Sadeque, A.J., Wandel, C., He, H., Shah, S., Wood, A.J., 2000. Increased drug delivery to the brain by P-glycoprotein inhibition. Clin. Pharmacol. Therap. 68, 231–237.
Schinkel, A.H., Wagenaar, E., Mol, C.A., van Deemter, L., 1996. P-glycoprotein in the blood-brain barrier of mice influences the brain penetration and pharmacological activity of many drugs. J. Clin. Invest. 97, 2517–2524.
Schuster, D., Laggner, C., Langer, T., 2005. Why drugs fail – a study on side effects in new chemical entities. Curr. Pharma. Des. 11, 3545–3559.
Shafer, T.J., Rijal, S.O., Gross, G.W., 2008. Complete inhibition of spontaneous activity in neuronal networks in vitro by deltamethrin and permethrin. Neurotoxicology 29, 203–212.
Sieber, M., Hoffmann, D., Adler, M., Vaidya, V.S., Clement, M., et al., 2009. Comparative analysis of novel noninvasive renal biomarkers and metabonomic changes in a rat model of gentamicin nephrotoxicity. Toxicol. Sci.: Off. J. Soc. Toxicol. 109, 336–349.
Siflinger-Birnboim, A., Del Vecchio, P.J., Cooper, J.A., Blumenstock, F.A., Shepard, J.M., Malik, A.B., 1987. Molecular sieving characteristics of the cultured endothelial monolayer. J. Cell. Physiol. 132, 111–117.
Smirnova, L., Hogberg, H.T., Leist, M., Hartung, T., 2014. Developmental neurotoxicity – challenges in the 21st century and in vitro opportunities. ALTEX 31, 129–156.
Sturm, M., Bertsch, A., Gropl, C., Hildebrandt, A., Hussong, R., et al., 2008. OpenMS – an open-source software framework for mass spectrometry. BMC Bioinform. 9, 163.
Sugimoto, S., Yamamoto, Y.L., Nagahiro, S., Diksic, M., 1995. Permeability change and brain tissue damage after intracarotid administration of cisplatin studied by double-tracer autoradiography in rats. J. Neuro-oncol. 24, 229–240.
Tyan, S.H., Shih, A.Y., Walsh, J.J., Maruyama, H., Sarsoza, F., et al., 2012. Amyloid precursor protein (APP) regulates synaptic structure and function. Mol. Cell. Neurosci. 51, 43–52.
Valdivia, P., Martin, M., LeFew, W.R., Ross, J., Houck, K.A., Shafer, T.J., 2014. Multi-well microelectrode array recordings detect neuroactivity of ToxCast compounds. Neurotoxicology 44, 204–217.
van Vliet, E., Morath, S., Eskes, C., Linge, J., Rappsilber, J., et al., 2008. A novel in vitro metabolomics approach for neurotoxicity testing, proof of principle for methyl mercury chloride and caffeine. Neurotoxicology 29, 1–12.
Vandormael, B., Fourla, D.D., Gramowski-Voss, A., Kosson, P., Weiss, D.G., et al., 2011. Superpotent [Dmt(1)] dermorphin tetrapeptides containing the 4-aminotetrahydro-2-benzazepin-3-one scaffold with mixed mu/delta opioid receptor agonistic properties. J. Med. Chem. 54, 7848–7859.
Vogelstein, B., Lane, D., Levine, A.J., 2000. Surfing the p53 network. Nature 408, 307–310.
Wanek, T., Mairinger, S., Langer, O., 2013. Radioligands targeting P-glycoprotein and other drug efflux proteins at the blood–brain barrier. J. Label. Comp. Radiopharma. 56, 68–77.
Wang, H., Qian, W.J., Mottaz, H.M., Clauss, T.R., Anderson, D.J., et al., 2005. Development and evaluation of a micro- and nanoscale proteomic sample preparation method. J. Proteome Res. 4, 2397–2403.
Waterman-Storer, C.M., Karki, S.B., Kuznetsov, S.A., Tabb, J.S., Weiss, D.G., et al., 1997. The interaction between cytoplasmic dynein and dynactin is required for fast axonal transport. Proc. Natl. Acad. Sci. USA 94, 12180–12185.
Weiss, D.G., 2011. Neurotoxicity assessment by recording electrical activity from neuronal networks on microelectrode array neurochips. In: Aschner, M., Suñol, C., Bal-Price, A. (Eds.), Cell Culture Techniques. Humana Press, New York, pp. 467–480.
West, P.R., Weir, A.M., Smith, A.M., Donley, E.L., Cezar, G.G., 2010. Predicting human developmental toxicity of pharmaceuticals using human embryonic stem cells and metabolomics. Toxicol. Appl. Pharm. 247, 18–27.
Wilmes, A., Limonciel, A., Aschauer, L., Moenks, K., Bielow, C., et al., 2013. Application of integrated transcriptomic, proteomic and metabolomic profiling for the delineation of mechanisms of drug induced cell stress. J. Proteomics 79, 180–194.
Zhao, W., Mosley, B.S., Cleves, M.A., Melnyk, S., James, S.J., Hobbs, C.A., 2006. Neural tube defects and maternal biomarkers of folate, homocysteine, and glutathione metabolism. Birth defects research Part A. Clin. Mol. Teratol. 76, 230–236.
Zurich, M.G., Honegger, P., 2011. Ochratoxin A at nanomolar concentration perturbs the homeostasis of neural stem cells in highly differentiated but not in immature three-dimensional brain cell cultures. Toxicol. Lett. 205, 203–208.
Zurich, M., Bal-Price, A., 2015. Potential biomarkers of neurotoxicity identified by transcriptomics analyses in 3D rat brain aggregating cultures after repeated exposure to 12 drugs (in preparation).
Zurich, M.-G., Stanzel, S., Kopp-Schneider, A., Prieto, P., Honegger, P., 2013. Evaluation of aggregating brain cell cultures for the detection of acute organ-specific toxicity. Toxicol. In Vitro 27, 1416–1424.